

## Dynamics of cross relaxation in nuclear magnetic double resonance\*

D. E. Demco,<sup>†</sup> J. Tegenfeldt,<sup>‡</sup> and J. S. Waugh

Department of Chemistry, Massachusetts Institute of Technology, Cambridge, Massachusetts 02139

(Received 7 October 1974)

A theory, based on the formalism of memory functions, is developed to describe the rate of thermal mixing  $T_{IS}^{-1}$  between two spin species, one abundant and one dilute, in double-resonance experiments on solids. Cross-polarization spectra (dependence of  $T_{IS}^{-1}$  on departure of rf field strength from conditions for resonant mutual spin flip) are computed for  $\text{CaF}_2$  in two experimental limits: one where the abundant species is spin locked and the other where it is demagnetized in the rotating frame. Results for the latter case are successfully compared with experimental data of McArthur *et al.* Modifications expected from introduction of a third (abundant) species are discussed. An alternative theory, based on information theory, is also presented.

### I. INTRODUCTION

The term "spin dynamics" refers to the processes by which a system of spins, subject to some internal interactions but isolated from other degrees of freedom (the "lattice"), proceeds from an experimentally realizable but otherwise arbitrary initial state toward a final state of (presumed) thermodynamic equilibrium. This progress is imagined to be monitored by means of measurable macroscopic quantities such as magnetizations or energies. Because the time dependence  $f(t)$  of any such quantity can always be formally represented through a Fourier transform as a generalized spectral response function  $\hat{f}(\omega)$ , discussions of these phenomena can be cast in the language either of relaxation or of line shapes. The richness of phenomena which can be exposed in magnetic resonance experiments has led to an enormous theoretical literature on spin dynamics since the early phenomenological description of Bloch<sup>1</sup> and the moment expansions from first principles of Van Vleck.<sup>2</sup>

The present paper is concerned with a particular situation of current experimental interest, one in which two different species of nuclear spins, one (I) abundant and the other (S) dilute, come to mutual equilibrium through a process of cross relaxation in a time denoted by  $T_{IS}$ . Our direct motivation is connected with a desire to understand and design optimal experimental procedures which exploit this cross relaxation to enhance the sensitivity with which the NMR spectrum of the rare spins can be detected. Such detection can be made indirectly<sup>3-7</sup> by observing the loss of I-spin order when the S-spin resonance is excited, or directly<sup>8,9</sup> by observing S-spin magnetization transmitted from the I spins. While an understanding of the cross-relaxation process is indispensable to both, we shall emphasize the point of view appropriate to the latter. In a typical experiment, the I spins, having first been brought to their equilibrium Curie magnetization  $M_{0I}$  by exposure to a strong field  $\vec{H}_0$  in the labo-

ratory, are brought to a spin-locked condition<sup>3,10</sup> in a resonant rf field  $H_{1I}$ , where they are characterized by a low Zeeman spin temperature in the rotating frame. By applying a second rotating field of strength  $H_{1S}$  at (or near) the S-spin Larmor frequency, a thermal contact is established,<sup>3,4</sup> and a common spin temperature is reached with time constant  $T_{IS}$ . This time depends in particular on the values of  $H_{1I}$  and  $H_{1S}$ , and is shortest when the Hartmann-Hahn condition<sup>3</sup>  $\gamma_I H_{1I} = \gamma_S H_{1S}$  is satisfied. When  $H_{1S}$  is made larger than this condition specifies, the equilibrium is slowed down, but at the same time the value of the S-spin magnetization is enhanced, since it depends on rf field and spin temperature  $\theta$  through Curie's law,  $M_S = C_S H_{1S} / \theta$ . Thus optimal design of an experiment may require departure from the Hartmann-Hahn condition, and requires a knowledge of the dependence of  $T_{IS}$  on  $H_{1S}$ . We shall refer to the variation of  $T_{IS}^{-1}$  with  $\omega_{1S} - \omega_{1I} = \gamma_S H_{1S} - \gamma_I H_{1I}$  as a *cross-polarization spectrum*.

Experimental and theoretical knowledge of such spectra is in a fragmentary state: Lang and Moran<sup>11</sup> have made some measurements, but in a system where the presence of a third (abundant) spin species complicates the situation (see below). McArthur, Hahn, and Walstedt<sup>5</sup> have made precise and detailed measurements in  $\text{CaF}_2$  crystals ( $I = {}^{19}\text{F}$ ,  $S = {}^{43}\text{Ca}$ ) in a slightly different regime: the I spins, before thermal contact, are adiabatically demagnetized in the rotating frame so that they are ordered only with respect to their local fields  $H'_{LI}$ .  $T_{IS}$  is then shortest when  $\gamma_I H'_{LI} \approx \gamma_S H_{1S}$ . McArthur *et al.*<sup>5</sup> have called the dependence of  $T_{IS}^{-1}$  on  $\omega_{1S}$  a "dipolar fluctuation spectrum." Experimentally they observed that over a very wide range this spectrum is *exponential*, i. e., is associated with an apparently *Lorentzian* time correlation function. Similar behavior has been observed in some organic solids.<sup>12,13</sup>

This remarkable result, quite apart from its significance for experimental design, calls for the-

oretical understanding. No theory has up to this point existed which attempts to predict the functional form of cross-polarization spectra. Hartmann and Hahn<sup>3</sup> accounted for the general magnitudes of  $T_{IS}$  by a perturbation-theory approach, invoking the spin-temperature hypothesis fully, and assuming *ad hoc* a Gaussian form for the correlation function of the fluctuating perturbation. Lurie and Slichter<sup>4</sup> adopted a somewhat similar approach, assuming a Gaussian  $I$ -spin "line shape" and a  $\delta$ -function shape for the  $S$ -spin. McArthur *et al.*,<sup>5</sup> analyzing their results for the case of adiabatic demagnetization in the rotating frame mentioned above, simply parametrized the experimentally observed exponential form of the cross-polarization spectrum by means of a moment analysis.

It is worth pointing out that cross-polarization spectra in double resonance experiments are of general theoretical interest because of the richness of different experimental regimes which can be realized, some of which are of greater theoretical tractability than cross-relaxation problems considered in the past.<sup>14-16</sup> The richness derives from the fact that properties, (e.g. heat capacities) of the two spin systems, regarded as thermodynamic entities, can be manipulated independently by application of rf magnetic fields, continuous or pulsed, at or near their respective Larmor frequencies. Similarly, the nature and strength of the effective coupling mechanism, as well as the initial states of  $I$  and  $S$  systems, can also be varied by the experimenter.

Exact calculation of the required correlation functions of dynamical variables is in general not possible for strongly coupled many-body systems; such calculation raises conceptual and mathematical difficulties typical of a certain class of many-body problems in which the "self-energy" effects due to the interaction are large compared to the "unperturbed single-particle energies." To overcome this difficulty two main approaches have been elaborated. One involves an attack on the microscopic problem from first principles, making appropriate mathematical approximations. A number of calculations of this type, applicable to spin systems, have been attempted.<sup>17-25</sup> In particular, the theories of Resibois and DeLeener<sup>18,19</sup> and recently Reiter,<sup>23-25</sup> among others based on an infinite-order perturbation expansion with selective resummation, have met with some success. Also, for the problem of the usual NMR absorption line shape, a theory based on a Dyson expansion has been successfully employed to calculate the short-time behavior of the free induction decay.<sup>26-29</sup> The correlation functions appropriate to the cross-polarization "line shape" are different, and, as we shall see, this procedure is no longer applicable.

The other procedure is to adopt what amounts to

a "fitting scheme"<sup>30-36</sup> in which one postulates a certain plausible and perhaps defensible shape (e.g., Gaussian) for some suitable function (e.g., a spin correlation function, a memory function, etc.) and adjusts parameters to fit certain rigorously calculable quantities such as moments. This procedure is esthetically less pleasing from a fundamental point of view, but may be very useful if it succeeds where other methods fail in predicting experimental results. We adopt this approach in the present work, within the framework of a memory-function formalism. We show that exact knowledge of a few moments, together with a Gaussian memory function, reproduces a wide variety of heretofore unexplained experimental results with great accuracy. An alternative calculation based on information theory,<sup>37,38</sup> is also presented.

## II. BASIC THEORY

### A. Hamiltonian and frame of reference

In this section we recall some details related to the double-resonance Hamiltonians and representative quantum-mechanical interaction representations for later reference. Special attention will be given to the relative magnitudes of different terms in the total Hamiltonian.

The most common spin system encountered in the double-resonance experiments<sup>3,4</sup> contains two spin species  $I$  and  $S$  with different magnetogyric ratios  $\gamma_I$  and  $\gamma_S$ . The sample, which contains  $N_I$  and  $N_S$  spins ( $N_I \gg N_S$ ), is placed in a large static magnetic field  $\vec{H}_0$ . The field  $\vec{H}_0$  is supposed to be along the  $Z$  axis. We discuss only the situations in which we may neglect the relative motions of the spins, and all the spin-lattice relaxation times of both spin species are taken to be infinitely long.

The high-field double-resonance<sup>3,4</sup> Hamiltonian in the laboratory reference frame is

$$\mathcal{H} = \mathcal{H}_I + \mathcal{H}_S + \mathcal{H}_{IS} + \mathcal{H}_{rf}(t) \quad (2.1)$$

The Hamiltonian  $\mathcal{H}_I$  is defined as

$$\mathcal{H}_I = \mathcal{H}_{ZI} + \mathcal{H}_{CI} + \mathcal{H}_{II} \quad (2.2)$$

where  $\mathcal{H}_{ZI} = -\omega_{0I}I_Z$ ,  $\omega_{0I} = \gamma_I H_0$  represents the Zeeman Hamiltonian,  $\mathcal{H}_{CI}$  is the chemical-shift Hamiltonian, and  $\mathcal{H}_{II}$  describes the magnetic interactions between  $I$  spins. In accordance with many experimental situations,<sup>39</sup> especially for protons,<sup>40</sup> the chemical-shift contribution to the total Hamiltonian of the abundant  $I$  spin is very small and can be disregarded.

The Hamiltonian  $\mathcal{H}_S$  which characterizes the dilute spin system is

$$\mathcal{H}_S = \mathcal{H}_{ZS} + \mathcal{H}_{CS} + \mathcal{H}_{SS} \quad (2.3)$$

where the terms have the same significance as in Eq. (2.2). Because we are interested in the be-

havior of spin systems on a time scale small compared with the spin-spin relaxation time of the  $S$  spins, we can neglect the term  $\mathcal{H}_{SS}$  in Eq. (2.3). This is also equivalent to considering the amplitude of the effective field applied to the dilute spin system to be much greater than the local field produced at one particular  $S$  spin by the other  $S$  spins. If high-resolution spectra of rare spins<sup>6-8</sup> are used for investigation of the double-resonance spin dynamics the chemical-shift (or Knight-shift) contribution to the Hamiltonian  $\mathcal{H}_S$  has to be taken into account. In this case the  $S$ -spin system consists of  $\alpha$  quasi-independent subsystems, where  $\alpha$  represents the number of resolved lines in the high-resolution spectrum. For each  $S$ -spin subsystem, without loss of generality, we can include the contribution of the chemical-shift Hamiltonian in the Zeeman term,  $\mathcal{H}_{ZS} = -\omega_{0S}S_Z$  ( $\omega_{0S} = \gamma_S H_0$ ).

The Hamiltonian  $\mathcal{H}_{IS}$  describes the interactions between  $I$  and  $S$  spin systems. If we consider the magnetogyric ratios  $\gamma_I$  and  $\gamma_S$  to be different, the last term of Eq. (2.1), which describes the interaction of the spin system with radio-frequency magnetic fields of amplitudes  $H_{1I}$  and  $H_{1S}$  and frequencies  $\omega_I$  and  $\omega_S$ , respectively, has the form

$$\mathcal{H}_{1I}(t) = -2\omega_{1I}I_X \cos\omega_I t - 2\omega_{1S}S_X \cos\omega_S t, \quad (2.4)$$

where  $\omega_{1I} = \gamma_I H_{1I}$  and  $\omega_{1S} = \gamma_S H_{1S}$ . The total spin operators are  $\vec{I} = \sum_i \vec{I}_i$  and  $\vec{S} = \sum_m \vec{S}_m$ . For convenience we have used in Eqs. (2.1)–(2.4) units in which  $\hbar = 1$ .

The time evolution of the statistical ensemble having an explicitly time-dependent Hamiltonian  $\mathcal{H}$  can be described by a density operator  $\rho(t)$  which satisfies the Liouville–von Neumann equation

$$i \frac{\partial \rho(t)}{\partial t} = [\mathcal{H}, \rho(t)]. \quad (2.5)$$

A solution of Eq. (2.5) can be obtained if we describe the statistical ensemble in a new quantum-mechanical representation defined by the canonical transformation

$$\rho_{TR}(t) = (TR)\rho(t)(TR)^\dagger, \quad (2.6)$$

where

$$R = R_I R_S, \quad R_I = e^{(-i\omega_I I_Z t)}, \quad R_S = e^{(-i\omega_S S_Z t)} \quad (2.7)$$

and

$$T = T_I T_S, \quad T_I = e^{(i\theta_I I_Y)}, \quad T_S = e^{(i\theta_S S_Y)}. \quad (2.8)$$

The canonical transformation defined by Eq. (2.8) tilts the  $\hat{Z}$  axes through the angles  $\theta_I = \tan^{-1}[\omega_{0I}/(\omega_{0I} - \omega_I)]$  and  $\theta_S = \tan^{-1}[\omega_{0S}/(\omega_{0S} - \omega_S)]$ . In the tilted rotating frames defined by Eqs. (2.6)–(2.8) the Hamiltonian of the  $I$ - $S$  spin system obtained from Eq. (2.5) is

$$\mathcal{H}_{TR} = (TR)\mathcal{H}(TR)^\dagger + i(\dot{TR})(TR)^\dagger. \quad (2.9)$$

A concrete expression for  $\mathcal{H}_{TR}$  can be obtained from Eqs. (2.9) and (2.1)–(2.4) in which we consider only pure dipolar couplings between the spins:

$$\mathcal{H}_{TR} = -\omega_{\text{eff},I} I_Z - \omega_{\text{eff},S} S_Z + P_2(\cos\theta_I)\mathcal{H}_{II}^0 + \mathcal{H}_{II}^{(\text{ns})} + \mathcal{H}_p, \quad (2.10)$$

where the effective frequencies are  $\omega_{\text{eff},I} = [\omega_{1I}^2 + \Delta\omega_I^2]^{1/2}$  and  $\omega_{\text{eff},S} = [\omega_{1S}^2 + \Delta\omega_S^2]^{1/2}$ , with  $\Delta\omega_I = \omega_{0I} - \omega_I$  and  $\Delta\omega_S = \omega_{0S} - \omega_S$ . The off-resonance parameters can also include the chemical-shift effect. In Eq. (2.10) the zero superscript indicates a truncation<sup>2</sup> or zero-order average<sup>41</sup> of the dipolar Hamiltonian

$$\mathcal{H}_{II}^0 = \sum_{i>j} b_{ij}(\vec{I}_i \cdot \vec{I}_j - 3I_{iz}I_{jz}), \quad (2.11)$$

with the interaction factor

$$b_{ij} = \gamma_I^2 \hbar r_{ij}^{-3} P_2(\cos\theta_{ij}),$$

The Hamiltonian  $\mathcal{H}_p$  originates from  $I$ - $S$  spin interaction and has the general form

$$\begin{aligned} \mathcal{H}_p = & \cos\theta_I \cos\theta_S \sum_{i,m} b_{im} I_{iz} S_{mz} + \sin\theta_I \sin\theta_S \sum_{i,m} b_{im} I_{ix} S_{mx} \\ & - \sin\theta_I \cos\theta_S \sum_{i,m} b_{im} I_{ix} S_{mz} \\ & - \cos\theta_I \sin\theta_S \sum_{i,m} b_{im} I_{iz} S_{mx}, \end{aligned} \quad (2.12)$$

with

$$b_{im} = -2\gamma_I \gamma_S \hbar r_{im}^{-3} P_2(\cos\theta_{im}).$$

In the above expressions the indices  $(i, j)$  and  $m$  refer to the  $I$  and  $S$  spins, respectively.  $r_{ij}$  is the distance between  $i$  and  $j$  spins.  $\theta_{ij}$  is the angle between the vector  $\vec{r}_{ij}$  connecting  $i$  and  $j$  spins and the applied magnetic field  $H_0 \hat{Z}$ .

The spin dynamics in a double-resonance experiment can be, in general, analyzed in two extreme conditions. The first corresponds to high effective fields and is realized by transferring Zeeman order of  $I$  spins from laboratory to rotating reference frame using spin locking (hereafter referred to as SL) procedures.<sup>10</sup> The second case corresponds to a low-effective-field condition for  $I$ -spins and is achieved by adiabatic demagnetization in the rotating frame<sup>42</sup> (hereafter referred to as ADRF).

In the SL case the nonsecular part of the dipolar Hamiltonian

$$\begin{aligned} \mathcal{H}_{II}^{(\text{ns})} = & \frac{3}{2} \sin^2 \theta_I \sum_{i>j} b_{ij} (I_{ix} I_{jz} + I_{iz} I_{jx}) \\ & - \frac{3}{2} \sin^2 \theta_I \sum_{i>j} b_{ij} (I_{ix} I_{jx} - I_{iy} I_{jy}) \end{aligned} \quad (2.13)$$

can be discarded in Eq. (2.10) by truncation.<sup>41</sup> This term is responsible for coupling between Zeeman and secular-dipolar  $I$ -spin reservoirs and establishment of a common spin temperature.<sup>15,16,43</sup> It is

now possible to separate the spin systems involved in a double-resonance experiment into two subsystems characterized by the Hamiltonians  $\mathcal{H}_1$  and  $\mathcal{H}_2$  defined by

$$\begin{aligned}\mathcal{H}_1 &= -\omega_{\text{eff},I}I_Z + P_2(\cos\theta_I)\mathcal{H}_{II}^0 \\ \mathcal{H}_2 &= -\omega_{\text{eff},S}S_Z,\end{aligned}\quad (2.14)$$

coupled by a Hamiltonian  $\mathcal{H}_p$  given in Eq. (2.12). The general form of  $\mathcal{H}_p$  makes it possible to discuss ADRF as a limiting case of the SL procedure for  $I$ -spin preparation. If  $H_{1I}$  is changed adiabatically from the value  $H_{1I} \gg H'_{LI}$  to the value  $H_{1I} \ll H'_{LI}$ , where  $H'_{LI}$  is the local field at the site of  $I$  spins in their rotating frame, the tilt angle  $\theta_I$  can be considered as approaching the value zero. Thus the Hamiltonians of interest in the ADRF case become from Eqs. (2.12)–(2.14)

$$\begin{aligned}\mathcal{H}_1 &= \mathcal{H}_{II}^0, \quad \mathcal{H}_2 = -\omega_{\text{eff},S}S_Z, \\ \mathcal{H}_p &= \cos\theta_S \sum_{i,m} b_{im}I_{iZ}S_{mZ} - \sin\theta_S \sum_{i,m} b_{im}I_{iZ}S_{mX}.\end{aligned}\quad (2.15)$$

Because  $N_I \gg N_S$  and/or  $\gamma_I \gg \gamma_S$ , the terms which are included in the  $\mathcal{H}_p$  Hamiltonians are smaller than either  $\mathcal{H}_1$  and  $\mathcal{H}_2$  and can be considered as perturbations. This imposes a further restriction to the amplitude of the effective magnetic fields applied to the  $S$  spins in the sense that  $H_{\text{eff},S}$  has to be large compared with the local field at the site of dilute spins determined by  $I$ - $S$  interaction in the rotating frame. For such a small coupling between the subsystems the secular cross-coupling dipolar term  $\sum_{i,m} b_{im}I_{iZ}S_{mZ}$  can be arbitrarily associated with the Hamiltonians  $\mathcal{H}_p$ . These Hamiltonians, Eqs. (2.12)–(2.15), are very general in the sense that they contain terms which induce multiple quantum transitions<sup>44–46</sup> in the low and high orders of perturbation.

We remark that the forms of the above Hamiltonians, Eqs. (2.12), (2.14), and (2.15), will be different in the intermediate effective field condition,  $H_{\text{eff},I} \sim H'_{LI}$ , or if the abundant spin system is subjected to a periodic external perturbation in the form of intense radio-frequency pulses. In the last case the  $I$ -spin system can be properly described by a time-independent average Hamiltonian<sup>47</sup> and a spin temperature<sup>48</sup> in a frame of reference defined by the external perturbation.

The presence of quadrupolar interactions for  $I$  and/or  $S$  spins in the Hamiltonian of Eq. (2.1) will introduce new features of double-resonance dynamics, especially in low-field conditions or where nearly degenerate transitions exist for other reasons. A detailed analysis of this case will be reported elsewhere.

### B. Spin dynamics

The spin systems which participate in a double-

resonance experiment can be described by their thermodynamic coordinates which are represented by the quantum-mechanical average of the observable operators. The time evolution of the thermodynamic coordinates as a function of the conditions of experimental preparation and the physical characteristics of the subsystems can be obtained from the Liouville–von Neumann equation, Eqs. (2.5) and (2.6), for the density operator of the whole system. This can be done by using very general quantum-mechanical theories<sup>49–56</sup> formulated in the following manner: (a) Both subsystems described by quantum-mechanical operators are treated in a symmetrical way. (b) No statistical assumption is made about the subsystems in interaction. In particular, the relative “size” of the spin systems can be arbitrary and their states can deviate arbitrarily from thermodynamic equilibrium. Also the assumption of an instantaneous canonical distribution description for the subsystems is not involved. (c) The coupling between the subsystems is not necessarily a small perturbation.

In a double-resonance experiment the subsystems are represented by  $I$ - and  $S$ -spin systems. The thermodynamic coordinates<sup>55</sup> are defined by the quantum-mechanical averages of the operators,

$$\langle \mathcal{H}_1 \rangle_t = \text{Tr}\{\mathcal{H}_1 \rho_{TR}(t)\}, \quad \langle \mathcal{H}_2 \rangle_t = \text{Tr}\{\mathcal{H}_2 \rho_{TR}(t)\}, \quad (2.16)$$

where  $\mathcal{H}_1$  and  $\mathcal{H}_2$  are given by Eqs. (2.14) or (2.15). From the definition of the thermodynamic coordinates, Eq. (2.16), it follows that the short- and long-time-scale behavior of the system are to be described in the tilted-rotating-frames interaction representation. To observe the macroscopic variables it is necessary to switch from tilted rotating frames to the observation reference frames which are represented by conventional rotating frames. In the indirect<sup>3–7</sup> procedure of double resonance the signal detected in the rotating reference frame of the abundant  $I$ -spin system is proportional to the Zeeman<sup>3</sup> or dipolar<sup>4</sup> energy described by the  $\langle \mathcal{H}_1 \rangle_t$  coordinate. The time evolution of Zeeman coordinate  $\langle \mathcal{H}_2 \rangle_t$  can be observed using the direct-detection version of double resonance<sup>8</sup> in the rotating reference frame of the dilute spins. All these explain requirement (a) of the theory.

The  $I$ -spin subsystem is generally represented by an abundant spin system with strong internal interactions. The large heat capacity of the  $I$ -spin system compared with the  $S$ -spin subsystem, fast correlation, and fast-spin diffusion approximations<sup>5</sup> will make the abundant spin system behave as a thermal bath, characterized by a spin temperature. The presence of molecular motion<sup>3,57</sup> or the reduction of  $I$ - $I$  spin interaction by coherent radio-frequency perturbation<sup>47</sup> will radically change the statistical properties of the  $I$ -spin system by re-

ducing its heat capacity and increasing the correlation time which characterizes its dissipative behavior. Condition (b) is also related to the fact that for the dilute spin system during the irreversible exchange of energy with the  $I$ -spin system an instantaneous canonical distribution and an instantaneous spin temperature cannot be defined. Because the coupling between  $S$  spin is very small compared with  $I$ - $S$  cross coupling, the time evolution of the off-diagonal elements of the reduced density matrix operator of the dilute spins will decay on a time scale comparable with diagonal elements. This fact prevents us from treating the dynamics of spin systems by using a thermodynamic model based on the spin-temperature formalism.

The last condition (c) would permit the analysis of spin dynamics in the cases of moderately dilute spins, relative strong coupling, low-effective-fields, or multiple-spin transitions.

An exact kinetic equation for the thermodynamic coordinates defined by Eq. (2.16) has been derived in an elegant manner using orthogonal operator expansion<sup>58</sup> and projection-operator technique<sup>49,50</sup> by Shimizu.<sup>55</sup> A natural choice of the orthogonal operators is in our case  $\mathcal{H}_1$  and  $\mathcal{H}_2$  defined by Eqs. (2.14) and (2.15). The orthogonality of the operators is defined in the following sense:

$$\text{Tr} \{ \mathcal{H}_1 \mathcal{H}_2 \} = 0 . \quad (2.17)$$

The density operator in the tilted rotating reference frame, Eq. (2.6), can be expanded using the projection operator technique:

$$\rho_{TR}(t) = P \rho_{TR}(t) + (1-P) \rho_{TR}(t) . \quad (2.18)$$

The projection operator  $P$  ( $P^2 = P$ ) on the subspaces defined by the Hamiltonian operators  $\mathcal{H}_1$  and  $\mathcal{H}_2$  is

$$P = \frac{\mathcal{H}_1}{\text{Tr} \{ \mathcal{H}_1^2 \}} \text{Tr} \{ \mathcal{H}_1 \dots \} + \frac{\mathcal{H}_2}{\text{Tr} \{ \mathcal{H}_2^2 \}} \text{Tr} \{ \mathcal{H}_2 \dots \} . \quad (2.19)$$

From Eqs. (2.5), (2.6), (2.9), (2.16), and (2.18), with a minimum amount of operator algebra, an exact kinetic equation for  $\langle \mathcal{H}_i \rangle_t$  ( $i = 1, 2$ ) which satisfies conditions (a)–(c) can be obtained:

$$\begin{aligned} \frac{\partial}{\partial t} \langle \mathcal{H}_i \rangle_t &= -i \text{Tr} \{ \mathcal{H}_i \hat{\mathcal{H}}_{TR} P \rho_{TR}(t) \} - i \text{Tr} \{ \mathcal{H}_i \hat{\mathcal{H}}_{TR} \hat{S}(t) \\ &\times (1-P) \rho_{TR}(0) \} - \int_0^t dt' \text{Tr} \{ \mathcal{H}_i \hat{\mathcal{H}}_{TR} \hat{S}(t-t') \\ &\times (1-P) \hat{\mathcal{H}}_{TR} P \rho_{TR}(t') \} , \end{aligned} \quad (2.20)$$

where the propagator  $\hat{S}(t)$  is

$$S(t) = e^{-i(1-P)\hat{\mathcal{H}}_{TR}t} , \quad (2.21)$$

and we shall denote a Liouville operator corresponding to an operator  $O$  by  $\hat{O}$ . The operator  $(1-P)\hat{\mathcal{H}}_{TR}$  in (2.21) is a Liouville operator, although not written as such for typographical reasons. These operators operate in the space of

operators rather than states of a system, i.e.,  $\hat{O}\rho(t) = [O, \rho(t)]$  and  $e^{-t\hat{O}}\rho(t) = e^{-tO}\rho(t) e^{tO}$ .

If we suppose that  $[\mathcal{H}_1, \mathcal{H}_2] = 0$ , the first inhomogeneous term in the right-hand side of Eq. (2.20) vanishes. The second inhomogeneous term of the integro-differential equation (2.20) is connected with the initial conditions and is, in general, different from zero. In the study of double-resonance spin dynamics the systems can be prepared initially in different conditions. For this reason an analysis of the inhomogeneous term behavior as a function of statistical properties of the subsystems and initial conditions has to be done. We suppose first that an arbitrary coupling between spin subsystems exists. In this case the second inhomogeneous term is different from zero for the functional form of experimental interest for  $\rho_{TR}(0)$ . To analyze the nonpathological case of small coupling it is more convenient to rewrite the propagator  $S(t)$ , Eq. (2.21), in the following form:

$$S(t) = S_0(t) S_p(t) , \quad (2.22)$$

where

$$S_0(t) = \exp[-i(\mathcal{H}_1 + \mathcal{H}_2)t] , \quad (2.23)$$

$$S_p(t) = T \exp \left( -i \int_0^t dt' [\mathcal{H}_p(t') - (P\mathcal{H}_{TR})(t')] \right) , \quad (2.24)$$

with

$$\mathcal{H}_p(t) - (P\mathcal{H}_{TR})(t) = \hat{S}_0^{-1}(t) (\mathcal{H}_p - P\mathcal{H}_{TR}) . \quad (2.25)$$

The Dyson time-ordering operator  $T$  orders operators of greater time arguments to the left-hand side. In the lowest Born approximation for the coupling Hamiltonian  $\mathcal{H}_p$  we can consider that  $S(t) \approx S_0(t)$ , and the second inhomogeneous term of Eq. (2.20) becomes

$$I_2(t) = i \text{Tr} \{ (\mathcal{H}_p \mathcal{H}_i) \hat{S}_0(t) (1-P) \rho_{TR}(0) \} . \quad (2.26)$$

Assuming now that the spin systems are prepared so that the initial density operator has a high-temperature canonical form

$$\rho_{TR}(0) \approx (1 - \beta_1 \mathcal{H}_1 - \beta_2 \mathcal{H}_2) / \text{Tr} \{ 1 \} , \quad (2.27)$$

where  $\beta_1$  and  $\beta_2$  are inverse spin temperatures, it is easy to prove that  $I_2(t) = 0$ . This is, in general,<sup>59</sup> the case in double-resonance experiments in which a saturating radio-frequency irradiation is used<sup>5,57</sup> to prepare the dilute spins before they are put in contact with the  $I$ -spin system. If the high-temperature approximation is not valid<sup>60</sup> for the canonical form of  $\rho_{TR}(0)$ , the  $I_2(t)$  term is still zero. In the case in which the  $S$ -spin system is not initially described by a canonical distribution, but such a description is valid for the  $I$ -spin system, again  $I_2(t)$  term is zero if  $[\mathcal{H}_1, \mathcal{H}_2] = 0$  and  $\text{Tr} \{ \mathcal{H}_1, \mathcal{H}_p \} = 0$ . From Eqs. (2.12), (2.14), and (2.15) we can see that is indeed the case. Thus, as we will see, a simple

transport equation describes the long-time behavior of coupled spin systems which is not affected by the initial state of S-spins in the limit of weak coupling. Of course, a particular preparation would be helpful in the cross-relaxation-time measurements.

In the second-order approximation of the perturbation Hamiltonian, from Eqs. (2.20)–(2.26) and the above considerations, we have

$$\frac{\partial}{\partial t} \langle \mathcal{H}_i \rangle_t = - \int_0^t dt' \text{Tr} \{ \hat{\mathcal{H}}_i \hat{\mathcal{C}}_{TR} \hat{S}_0(t-t') \times (1-P) \hat{\mathcal{C}}_{TR} P \rho_{TR}(t') \} \quad (2.28)$$

This general equation describes the short- and long-time behavior of thermodynamic coordinates, through the generalized collision operator which is the kernel of the integral from the right-hand side of Eq. (2.28). We suppose now that the generalized collision operator can be characterized by the existence of a correlation time  $\tau_c$  defined mathematically such that this operator goes to zero for  $t \gg \tau_c$ . On the short-time scale, for which  $t \leq \tau_c$ , from Eq. (2.28), we have

$$\langle \mathcal{H}_i \rangle_t = \langle \mathcal{H}_i \rangle_0 - \int_0^t dt' \int_0^{t'} dt'' \text{Tr} \{ \hat{\mathcal{H}}_i \hat{\mathcal{C}}_{TR} \hat{S}_0(t'-t'') \times (1-P) \hat{\mathcal{C}}_{TR} P \exp[-i(\hat{\mathcal{H}}_1 + \hat{\mathcal{H}}_2)t''] \rho_{TR}(0) \} . \quad (2.29)$$

It is important to remark that this equation shows "memory" in the sense that the values of thermodynamic coordinates  $\langle \mathcal{H}_i \rangle_t$  at moment  $t$  depend on all earlier values. Also, the initial conditions of preparation are important and are involved through  $\langle \mathcal{H}_i \rangle_0$  and  $\rho_{TR}(0)$ .

If the fast-correlation assumption is introduced, for times  $t \gg \tau_c$  the limit in the integral of Eq. (2.28) can be replaced by infinity. Also, it is possible to replace  $\rho_{TR}(t')$  by  $\rho_{TR}(t)$  in Eq. (2.28). After the change of variable  $t-t' \rightarrow \tau$ , Eq. (2.28) becomes

$$\frac{\partial}{\partial t} \langle \mathcal{H}_i \rangle_t = - \int_0^\infty d\tau \text{Tr} \{ \hat{\mathcal{H}}_i \hat{\mathcal{C}}_{TR} \hat{S}_0(\tau) \times (1-P) \hat{\mathcal{C}}_{TR} P \rho_{TR}(t) \} . \quad (2.30)$$

Suppose now that we are interested in the cross-polarization dynamics of dilute spins.<sup>8</sup> From Eq. (2.30) the following equation can be written in this case

$$\frac{\partial}{\partial t} \langle \mathcal{H}_2 \rangle_t = \frac{\langle \mathcal{H}_2 \rangle_t}{\text{Tr} \{ \hat{\mathcal{C}}_{21}^2 \}} \int_0^\infty d\tau C(\mathcal{H}_2; \mathcal{H}_2; \tau) + \frac{\langle \mathcal{H}_1 \rangle_t}{\text{Tr} \{ \hat{\mathcal{C}}_{11}^2 \}} \int_0^\infty d\tau C(\mathcal{H}_2; \mathcal{H}_1; \tau) , \quad (2.31)$$

where the correlation functions are defined by

$$C(\mathcal{H}_2; \mathcal{H}_2; \tau) = \text{Tr} \{ (\hat{\mathcal{C}}_p \hat{\mathcal{H}}_2) \hat{S}_0(\tau) (\hat{\mathcal{C}}_p \hat{\mathcal{H}}_2) \} , \quad (2.32)$$

$$C(\mathcal{H}_2; \mathcal{H}_1; \tau) = \text{Tr} \{ (\hat{\mathcal{C}}_p \hat{\mathcal{H}}_2) \hat{S}_0(\tau) (\hat{\mathcal{C}}_p \hat{\mathcal{H}}_1) \} ,$$

and for which the following relation is valid:

$$\int_0^\infty d\tau [C(\mathcal{H}_2; \mathcal{H}_2; \tau) + C(\mathcal{H}_2; \mathcal{H}_1; \tau)] = 0 . \quad (2.33)$$

We can now define new thermodynamic coordinates by

$$\beta_1(t) = \langle \mathcal{H}_1 \rangle_t / \text{Tr} \{ \hat{\mathcal{C}}_1^2 \} , \quad \beta_2(t) = \langle \mathcal{H}_2 \rangle_t / \text{Tr} \{ \hat{\mathcal{C}}_2^2 \} , \quad (2.34)$$

which in the high-temperature approximation have the dimensions of inverse temperature ( $k=1$ ). For these formal inverse temperatures<sup>61</sup> the following equation is valid:

$$\frac{\partial \beta_2(t)}{\partial t} = \frac{\beta_1(t) - \beta_2(t)}{T_{IS}} , \quad (2.35)$$

where the transport parameter  $T_{IS}$  which characterizes the cross-relaxation process is

$$T_{IS}^{-1} = \frac{-1}{\text{Tr} \{ \hat{\mathcal{C}}_2^2 \}} \int_0^\infty d\tau \text{Tr} \{ (\hat{\mathcal{C}}_p \hat{\mathcal{H}}_2) \exp[-i(\hat{\mathcal{H}}_1 + \hat{\mathcal{H}}_2)\tau] \times (\hat{\mathcal{C}}_p \hat{\mathcal{H}}_2) \} . \quad (2.36)$$

The microscopic expressions for cross-relaxation times in SL and ADRF cases can now be easily obtained from the general equation (2.36), valid for  $\tau_c \ll T_{IS}$  and second order in the perturbation Hamiltonian. Using the particular forms of  $\mathcal{H}_1$ ,  $\mathcal{H}_2$ , and  $\mathcal{H}_p$  given in Sec. IIA we obtain for the SL case

$$T_{IS}^{-1} = \sin^2 \theta_S \cos^2 \theta_I M_{2,SI} J_Z(\omega_{eff,S}) + \frac{1}{2} \sin^2 \theta_S \sin^2 \theta_I M_{2,SI} \times [J_X(\omega_{eff,S} - \omega_{eff,I}) + J_X(\omega_{eff,S} + \omega_{eff,I})] , \quad (2.37)$$

and in a similar manner for the ADRF case<sup>5</sup>

$$T_{IS}^{-1} = \sin^2 \theta_S M_{2,SI} J_Z(\omega_{eff,S}) , \quad (2.38)$$

where  $M_{2,SI}$  is the Van Vleck<sup>2</sup> second moment of the magnetic-resonance line determined by the cross-coupling dipolar interaction. The spectral density functions which describe the fluctuations in the thermal bath represented by the abundant spin system are given by

$$J_X(\omega) = \int_0^\infty d\tau \cos \omega \tau C_X(\tau) ,$$

$$J_Z(\omega) = \int_0^\infty d\tau \cos \omega \tau C_Z(\tau) , \quad (2.39)$$

which are the real parts of the Fourier transforms of the dipolar fluctuation autocorrelation functions,

$$C_X(\tau) = \text{Tr} \left\{ \left( \sum_i b_i I_{iX} \right) \exp[-iP_2(\cos \theta_I) \hat{\mathcal{C}}_{II}^0 \tau] \times \left( \sum_i b_i I_{iX} \right) \right\} / \text{Tr} \left\{ \left( \sum_i b_i I_{iX} \right)^2 \right\} \quad (2.40)$$

and

$$C_Z(\tau) = \text{Tr} \left\{ \left( \sum_i b_i I_{iZ} \right) \exp[-iP_2(\cos\theta_I)\mathfrak{K}_{I\tau}^0] \right. \\ \left. \times \left( \sum_i b_i I_{iZ} \right) \right\} / \text{Tr} \left\{ \left( \sum_i b_i I_{iZ} \right)^2 \right\}. \quad (2.41)$$

The cross-coupling interaction factors  $b_k$  which appear as weight factors for individual spin operators in the macroscopic operators  $\sum_i b_i I_{iX}$  and  $\sum_i b_i I_{iZ}$  are short-hand notations for  $b_{km}$ . We assume that the dilute spins are magnetically equivalent and  $b_{km}$  is thus independent of  $m$ . The correlation times  $\tau_c$ , characteristic of these autocorrelation functions, are determined by the  $I$ - $I$  interactions and are of the same order of magnitude as the spin-spin relaxation time  $T_{2I}$ .

The autocorrelation functions defined in Eqs. (2.40) and (2.41) decay monotonically with time, which makes  $J_X(\omega)$  approach zero for  $\omega\tau_c \gg 1$ . Because in the high-effective-field SL case  $\omega_{\text{eff},S}$ ,  $\omega_{\text{eff},I} \gg \omega_{LI} \sim 1/T_{2I}$ , and  $\tau_c \sim T_{2I}$ , Eq. (2.37) can be rewritten to a good approximation

$$T_{1S}^{-1} = \frac{1}{2} \sin^2\theta_I \sin^2\theta_S M_{2,SI} J_X(\Delta\omega_{\text{eff}}), \quad (2.42)$$

where  $\Delta\omega_{\text{eff}} = \omega_{\text{eff},S} - \omega_{\text{eff},I}$ . The above equation is valid only for  $\theta_I$  values different from  $\theta_m = \cos^{-1}(1/\sqrt{3})$  at which memory effects in the thermal bath become important in the case of dipolar interactions. We remark parenthetically that the same result can be generated if we neglect in the general perturbation Hamiltonian, Eq. (2.12), the terms which oscillate with  $\omega_{\text{eff},I}$ ,  $\omega_{\text{eff},S}$ , and  $\omega_{\text{eff},I} + \omega_{\text{eff},S}$  frequencies in the double rotating reference frame.<sup>43</sup>

The formalism developed in this section can also be used for evaluation of the cross-relaxation time in the intermediate field case, in which the abundant spins are cooled by a partial adiabatic demagnetization in the rotating frame. Now  $\omega_{\text{eff},I}$  is of the same order of magnitude as  $\omega_{LI}$ , and a nonsecular contribution to the dipolar interaction, Eq. (2.13), has to be taken into account in the Hamiltonians which lead to the decay of autocorrelation functions.

An inspection of the formulas for cross-relaxation times shows that the experimental parameters are involved through the effective frequencies  $\omega_{\text{eff},S}$  and  $\Delta\omega_{\text{eff},I}$  and the angle between the average directions of the spin quantization axes. In the SL case the  $I$  and  $S$  rotating reference frames rotate with relative angular frequencies  $|\omega_I - \omega_S|$ , which have large values if  $\omega_I \neq \omega_S$ . An automatic average over the equatorial angles is performed in Eqs. (2.37) or (2.42) through the truncation procedure,<sup>41</sup> leaving only the dependence on azimuthal angles. The abundant spin system is ordered in the local fields in the ADRF case. A supplemental average over the local directions of the quantization axis is also automatically included in Eq. (2.15) and thus

in the cross-relaxation time expression Eq. (2.38).

The cross-coupling Van-Vleck second moment and the dipolar fluctuation autocorrelation functions make the cross-relaxation times dependent on microscopic parameters of the sample. Also, the high-resolution spectrum of cross relaxation times<sup>9,9</sup> is generated by the discrete (for a single crystal) or continuous (for a powder) changes in the tilted angle  $\theta_S$ ,  $M_{2,SI}$ , and spectral density functions.

In order to analyze the short-time behavior of spin-system thermodynamic coordinates, we consider that before these systems are put in contact they are in a thermodynamic quasiequilibrium state. This can be done by applying a saturation pulse to the  $S$ -spin system until the initial spin temperature is  $T_{Si} = \infty$  and the  $I$  spins are cooled to a spin temperature  $T_{Ii}$ . From Eqs. (2.12), (2.14), and (2.29), using the high-temperature approximation, the normalized magnetization developed along  $H_{\text{eff},S}$  at a particular moment of time  $\tau$  is

$$\frac{M_S(\tau)}{M_{S,\text{eq}}} = (1 + \epsilon_{SI}) M_{2,SI} \int_0^\tau dt_2 \int_0^{t_2} dt_1 \\ \times [\cos^2\theta_I \sin^2\theta_S \cos(\omega_{\text{eff},S} t_2) C_Z(t_2) \\ + \sin^2\theta_I \sin^2\theta_S \cos(\omega_{\text{eff},S} t_2) \cos(\omega_{\text{eff},I} t_2) \\ \times C_X(t_2)], \quad (2.43)$$

where  $M_S(\tau) = \text{Tr}\{\gamma_S \hbar S_Z \rho_{TR}(\tau)\}$ . Usually for the SL case we have  $\theta_I = \pi/2$  and from Eq. (2.43) we get

$$\frac{M_S(\tau)}{M_{S,\text{eq}}} = \frac{1}{2} \sin^2\theta_S (1 + \epsilon_{SI}) M_{2,SI} \int_0^\tau dt_1 \int_0^{t_1} dt_2 \\ \times [\cos(\omega_{\text{eff},S} + \omega_{\text{eff},I}) t_2 \\ + \cos(\omega_{\text{eff},S} - \omega_{\text{eff},I}) t_2] C_X(t_2). \quad (2.44)$$

If formally we make  $\omega_{\text{eff},I} \rightarrow 0$  and  $\theta_I \rightarrow 0$  in (2.43), the ADRF case is obtained:

$$\frac{M_S(\tau)}{M_{S,\text{eq}}} = \sin^2\theta_S (1 + \epsilon_{SI}) M_{2,SI} \int_0^\tau dt_1 \int_0^{t_1} dt_2 \\ \times \cos(\omega_{\text{eff},S} t_2) C_Z(t_2). \quad (2.45)$$

In the above equations  $M_{S,\text{eq}}$  represents the equilibrium magnetization obtained in the cross-polarization process<sup>8</sup> with  $I$  spins

$$M_{S,\text{eq}} = [1/(1 + \epsilon_{SI})] C_S H_{\text{eff},S} / T_{Ii}, \quad (2.46)$$

where  $C_S = \frac{1}{3} \gamma_S^2 \hbar^2 S(S+1) N_S$  is the Curie constant and  $\epsilon_{SI} = C_S H_{\text{eff},S}^2 / C_I H_{\text{eff},I}^2$  is the heat capacity ratio of  $S$ - and  $I$ -spin systems.

In this section the dynamics of the dilute spin system in a double-resonance experiment was mainly analyzed, but similar equations can be derived for the thermodynamic coordinates of the  $I$ -spin system. Our interest in the  $S$ -spin system is motivated by the fact that, if high-resolution spectral intensities of these spins are to be obtained

without distortion, the direct detection method<sup>6</sup> is called for when it can be used.

### III. EVALUATION OF CROSS-POLARIZATION SPECTRA AND TRANSIENT OSCILLATIONS

In the computation of cross-polarization dynamics one of the central statistical assumptions used in Sec. II was the fact that the abundant spin system can be considered as a thermal bath. A direct result of this is that the evaluation of the cross-relaxation time and the short-time behavior which is represented by transient oscillations in the rotating frame<sup>5</sup> is tantamount to calculating dipolar fluctuation autocorrelation functions  $C_X(\tau)$  and  $C_Z(\tau)$ , Eqs. (2.40) and (2.41), whose shapes depend on whether the  $I$  spins are in SL or ADRF conditions.

The fact that the functional dependence of the cross-relaxation rates on the effective frequencies  $\omega_{\text{eff},s}$  or  $\Delta\omega_{\text{eff}}$ , which we will call in general a cross-polarization spectrum, is different for high- and low-effective-field double-resonance experiments, can be seen for instance from Eq. (2.41). If a rotation of spin operators is performed using the unitary operator  $e^{(i\pi/2)I_y}$ , we get

$$C_Z(\tau) = \text{Tr} \left\{ \left( \sum_i b_i I_{iX} \right) \exp \left[ -i \left( -\frac{1}{2} \hat{\mathcal{C}}_{II}^0 + \hat{\mathcal{C}}_{II}^{(\text{ns})} \right) \tau \right] \right. \\ \left. \times \left( \sum_i b_i I_{iX} \right) \right\} / \text{Tr} \left\{ \left( \sum_i b_i I_{iX} \right)^2 \right\}, \quad (3.1)$$

where  $\hat{\mathcal{C}}_{II}^{(\text{ns})}$  is given by Eq. (2.13) with  $\theta_I = \pi/2$ . We can see now that the difference between functional forms of  $C_X(\tau)$  and  $C_Z(\tau)$  is, except for the time scaling, determined by the nonsecular dipolar Hamiltonian, which has the same order of magnitude as the secular part and provides a supplemental mechanism for dipolar fluctuation for the  $I$ -spin system in the ADRF condition. Therefore the presence of exchange interactions will differentially affect the shape of autocorrelation functions only through the dipolar Hamiltonian.

It is difficult to make any *a priori* guess relative to the functional shape of  $C_X(\tau)$  and  $C_Z(\tau)$  before any detailed theory for these correlation functions is elaborated. Nevertheless, we can remark that if formally we consider coefficients  $b_k$  to be constants independent of  $I$ -spin coordinates the  $C_X(\tau)$  function, Eq. (2.40), becomes the autocorrelation function for the free induction decay (FID) of  $I$  spins, but it is scaled in time by the  $P_2(\cos\theta_I)$  factor. The  $C_Z(\tau)$  function, Eq. (2.41), becomes independent of fluctuation in the dipolar system. In conclusion, at least for the ADRF case, the  $C_Z(\tau)$  shape essentially depends on the punctual character of  $I$ - $S$  coupling.

The time evaluation of the FID,

$$G(\tau) = \text{Tr} \{ I_X \exp[-i(\hat{\mathcal{C}}_{\text{Ising}} + \hat{\mathcal{C}}_{\text{ex}})\tau] I_X \} / \text{Tr} \{ I_X^2 \},$$

is determined by Ising and exchange parts of the dipolar Hamiltonian, Eq. (2.11), for which

$$[\hat{\mathcal{C}}_{\text{Ising}}, I_X] \neq 0 \quad \text{and} \quad [\hat{\mathcal{C}}_{\text{ex}}, I_X] = 0. \quad (3.2)$$

Based on Eq. (3.2), if a Dyson expansion<sup>26</sup> is used, the zeroth-order approximation for FID is

$$G^{(0)}(\tau) = \text{Tr} \{ I_X \exp(-i\hat{\mathcal{C}}_{\text{Ising}}\tau) I_X \} / \text{Tr} \{ I_X^2 \},$$

which, mainly because of the form of  $\hat{\mathcal{C}}_{\text{Ising}}$ , is close to a Gaussian. In the case of the SL autocorrelation function we have

$$[\hat{\mathcal{C}}_{\text{Ising}}, \sum_i b_i I_{iX}] \neq 0 \quad \text{and} \quad [\hat{\mathcal{C}}_{\text{ex}}, \sum_i b_i I_{iX}] \neq 0, \quad (3.3)$$

which makes a Dyson expansion less justifiable. Nevertheless, using the limiting property of  $C_X(\tau)$  when  $b_i$  becomes a constant and for short time ( $\tau \ll \tau_c$ ), we can write the approximation

$$C_X^{(0)}(\tau) = \text{Tr} \left\{ \left( \sum_i b_i I_{iX} \right) \exp[-iP_2(\cos\theta_I)\hat{\mathcal{C}}_{\text{Ising}}\tau] \right. \\ \left. \times \left( \sum_i b_i I_{iX} \right) \right\} / \text{Tr} \left\{ \left( \sum_i b_i I_{iX} \right)^2 \right\}.$$

Of course this is a very rough approximation for  $C_X(\tau)$  and will give an incorrect second moment. Even so, a direct evaluation of  $C_X^{(0)}(\tau)$  for a CaF<sub>2</sub> single crystal shows a shape close to a Gaussian. As we shall see, for longer times, in spite of Eq. (3.3), the functional forms of  $C_X(\tau)$  and FID are similar and consequently less dependent on the punctual character of cross coupling.

#### A. Memory-function approach

Mori<sup>52</sup> and more recently Lado *et al.*<sup>22</sup> have shown that an exact equation of motion for the time-dependent correlation functions  $C(\tau)$  of a statistical system can be derived on the assumption of small displacements from equilibrium,

$$\frac{dC(\tau)}{d\tau} = i\Omega_0 C(\tau) - \int_0^\tau dt K(\tau-t)C(t), \quad (3.4)$$

where  $\Omega_0$  is the first moment of spectral density related to  $C(\tau)$  and  $K(t)$  is a *memory function*. In our case the dipolar fluctuation autocorrelation functions  $C_\alpha(\tau)$  ( $\alpha = X, Z$ ) are even functions of time and Eq. (3.4) reduces to

$$\frac{dC_\alpha(\tau)}{d\tau} = - \int_0^\tau dt K_\alpha(\tau-t)C_\alpha(t). \quad (3.5)$$

In the absence of calculations of the  $C_\alpha(\tau)$  from first principles a quite successful approach in practice is to assume a plausible shape (containing a number of adjustable parameters) for the memory function.<sup>22,35</sup>

On general grounds<sup>52</sup> it can be shown that the decay time of the memory function is of the same order of magnitude as or smaller than that of the cor-

relation function. Consequently, any short-time approximation for  $K_\alpha(t)$  will give a better long-time behavior for  $C_\alpha(\tau)$ . Moreover, in the *short-time* region the memory function appears to have a simpler structure than the correlation function itself. To analyze the range of validity of the above assumption let us define an autocorrelation vector in the same spirit as in the extended Mori theory for dynamical variables<sup>62</sup>:

$$\vec{C}_\alpha(\tau) = \begin{pmatrix} C_\alpha^{(0)}(\tau) \\ C_\alpha^{(2)}(\tau) \\ \vdots \\ C_\alpha^{(2m)}(\tau) \\ \vdots \end{pmatrix}, \quad (3.6)$$

where  $C_\alpha^{(2m)}(\tau)$  is one of the autocorrelation functions defined by Eqs. (2.40) and (2.41), but for the dynamical variables  $(d^{2m}/d\tau^{2m})[\sum_i b_i I_{i\alpha}(\tau)]$ , with  $\alpha = X, Z$  and  $C_\alpha^{(0)}(\tau) \equiv C_\alpha(\tau)$ . It is easy to prove that the autocorrelation vector satisfies the equation

$$\frac{d\vec{C}_\alpha(\tau)}{d\tau} = -\int_0^\tau dt \vec{K}_\alpha(\tau-t) \vec{C}_\alpha(t), \quad (3.7)$$

where  $\vec{K}_\alpha(t)$  is the memory-function vector associated with  $\vec{C}_\alpha(\tau)$ . From a knowledge of the analytical properties of the vector  $\vec{C}_\alpha(\tau)$ , it can be shown that the memory-function vector is an even function of time and has a finite initial value. Consequently, from a moment expansion for  $\vec{C}_\alpha(\tau)$  and  $\vec{K}_\alpha(t)$  with Eq. (3.7) the following relations between the moments  $M_{2n}^{(2m)}$  and  $N_{2n}^{(2m)}$  of  $C_\alpha^{(2m)}(\tau)$  and  $K_\alpha^{(2m)}(t)$ , respectively, are obtained:

$$\begin{aligned} K_\alpha^{(2m)}(0) &= M_2^{(2m)}, \\ N_2^{(2m)} &= M_2^{(2m)} [M_4^{(2m)} / (M_2^{(2m)})^2 - 1], \\ N_4^{(2m)} &= (M_6^{(2m)})^2 / (M_2^{(2m)})^3 - 2M_4^{(2m)} / (M_2^{(2m)})^2 + 1, \\ N_6^{(2m)} &= (M_2^{(2m)})^3 \left[ \frac{M_4^{(2m)}}{(M_2^{(2m)})^4} - \frac{3M_6^{(2m)}}{(M_2^{(2m)})^3} \right. \\ &\quad \left. + \left( 3 - \frac{M_4^{(2m)}}{(M_2^{(2m)})^2} \right) \frac{M_4^{(2m)}}{(M_2^{(2m)})^2} - 1 \right], \text{ etc.} \end{aligned} \quad (3.8)$$

Also the moments of  $C_\alpha^{(2m)}(\tau)$  functions can be related to those of  $C_\alpha^{(0)}(\tau)$  by

$$M_{2n}^{(2m)} / (M_2^{(2m)})^n = M_{2n}^{(0)} / (M_2^{(0)})^{n-1} / (M_{2(m+1)}^{(0)})^n. \quad (3.9)$$

Let us consider now two normalized correlation functions, a Gaussian,  $e^{-\tau^2/\tau_c^2}$ , and a Lorentzian,  $(1 + \tau^2/\tau_c^2)^{-1}$ , for which the moments up to any order can be exactly computed. In order to test the sensitivity of memory-function vector components to the functional form of  $C_\alpha^{(0)}(\tau)$  we have plotted, in Fig. 1,  $N_4^{(2m)} / (N_2^{(2m)})^2$  and  $N_6^{(2m)} / (N_2^{(2m)})^3$  versus  $m$

obtained from Eqs. (3.8) and (3.9) for Gaussian and Lorentzian input functions. From Fig. 1 we see that  $K_\alpha^{(0)}(t)$  and  $K_\alpha^{(2)}(t)$  are close to a Gaussian function, i. e.,

$$K_\alpha^{(0)}(t) = K_\alpha^{(0)}(0) e^{-\delta t^2}, \quad (3.10)$$

where  $\delta = (\frac{1}{2})N_2^{(0)}$ . For the  $m$ th ( $m > 1$ ) component of the memory-function vector which *automatically* incorporates  $M_{2(m+1)}^{(0)}$ , the Gaussian approximation is no longer valid. Because the higher-order components of  $\vec{K}_\alpha^{(0)}(t)$  are related to the long-time behavior of  $C_\alpha^{(0)}(\tau)$ , through the higher-order moments, we can see that the Gaussian approximation, Eq. (3.10), holds only for the *short-time* scale,  $\tau \leq (2/N_2^{(0)})^{1/2}$ .

Generally the initial time derivatives of the time-dependent autocorrelation functions, which are related to the moments of the corresponding spectral density functions by the relation  $M_{2n}^{(0)} = (-1)^n d^{2n} \times C_\alpha^{(0)}(\tau) / d\tau^{2n} |_{\tau=0}$ , can be calculated exactly since they can be expressed as equilibrium average properties of the system of interest. However, the calculation of these moments involves the evaluation of the traces of the squares of some complicated quantum-mechanical operators, and there is no general systematic pattern for evaluating the double sums involved in different types of particle-interaction terms. This fact makes difficult the calculation of the moments other than the second and fourth. That is one of the main reasons why we consider here the solution of Eq. (3.5) with a Gaussian approximation for the memory-function, Eq. (3.10). Using Laplace transforms, i. e.,

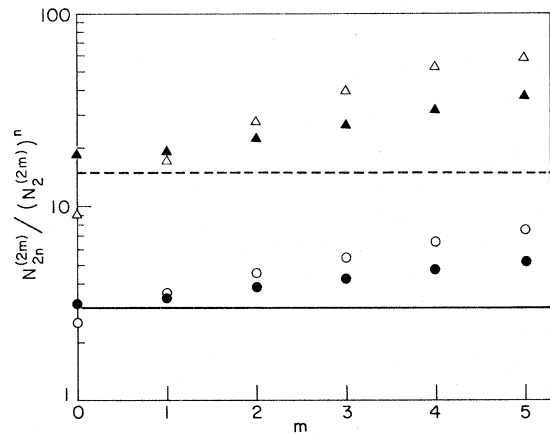


FIG. 1 Ratios  $N_{2n}^{(2m)} / (N_2^{(2m)})^n$  for the moments of the  $m$ th component of the memory-function vector vs  $m$  for a Gaussian (open circles and open triangles correspond to  $n=2$  and  $n=3$ , respectively) and a Lorentzian (full circles and full triangles correspond to  $n=2$  and  $n=3$ , respectively) autocorrelation function. For a Gaussian memory-function vector,  $N_4^{(2m)} / (N_2^{(2m)})^2 = 3$  (continuous line) and  $N_6^{(2m)} / (N_2^{(2m)})^3 = 15$  (dashed line).

$$\underline{C}_\alpha(z) = \int_0^\infty dt e^{-zt} C_\alpha(t), \quad (3.11)$$

where  $\text{Re} \underline{C}_\alpha(z) = J_\alpha(\omega)$ , the formal solution of Eq. (3.5) is

$$\underline{C}_\alpha(z) = 1/[z + \underline{K}_\alpha(z)]. \quad (3.12)$$

From Eqs. (2.39) and (3.12) a general expression for spectral density functions can be derived<sup>22</sup>:

$$J_\alpha(\omega) = K'_\alpha(\omega) / \{ [\omega - K''_\alpha(\omega)]^2 + [K'_\alpha(\omega)]^2 \}, \quad (3.13)$$

where  $K'_\alpha(\omega)$  and  $K''_\alpha(\omega)$  are the real and imaginary parts of the memory-function Fourier transform.

With the approximation, Eq. (3.10), we have

$$\begin{aligned} K'_\alpha(\omega) &= K_\alpha(0) \int_0^\infty dt e^{-\delta t^2} \cos \omega t, \\ K''_\alpha(\omega) &= K_\alpha(0) \int_0^\infty dt e^{-\delta t^2} \sin \omega t, \end{aligned} \quad (3.14)$$

where  $\delta$  depends on the autocorrelation type through the corresponding moments. In this form, a knowledge of the second and fourth moments leads directly from Eqs. (3.14), (3.13), (2.38), (2.42), (2.44), and (2.45) to the microscopic expressions

TABLE I. Definition of the lattice sums involved in the calculation of the moments  $M_2$  and  $M_4$  associated with dipolar fluctuation autocorrelation functions, Eqs. (2.40) and (2.41), and their values evaluated by computer for CaF<sub>2</sub>-type structures for different directions of  $\vec{H}_0$ . The units of  $b_i$  and  $b_{ij}$  coefficients are, respectively,  $\gamma_I \gamma_S \bar{n} / a^3$  and  $\gamma_I^2 \bar{n} / a^3$ , where  $a$  is the shortest fluorine-fluorine distance in CaF<sub>2</sub>.

Lattice sums	Direction of $\vec{H}_0$		
	[100]	[110]	[111]
$S_1 = \sum_i b_i^2$	1.554	20.33	26.46
$S_2 = \sum_i b_{ij}^2$	30.01	11.36	5.137
$S_3 = \sum_i b_{ij}^4$	182.7	14.16	1.190
$S_4 = \sum_{i < j} b_{ij}^2 b_i b_j$	9.985	22.32	0.311
$S_5 = \sum_{i < j} b_{ij}^4 b_i b_j$	55.25	55.59	0.177
$S_6 = \sum_{i < j} b_{ij}^2 b_{ik} b_{jk}$	40.31	10.83	1.803
$S_7 = \sum_{i \neq j \neq k} b_{ij}^2 b_{ik}^2 b_j^2$	1116	2322	666.8
$S_8 = \sum_{i \neq j \neq k} b_{ij}^2 b_{ik}^2 b_{jk} b_j$	488.7	395.8	2.841
$S_9 = \sum_{i \neq j \neq k} b_{ij}^2 b_{ik}^2 b_{jk} b_k$	133.1	-44.30	-11.40
$S_{10} = \sum_{i \neq j \neq k} b_{ij}^2 b_{jk}^2 b_{ik} b_k$	125.3	438.1	95.39
$S_{11} = \sum_{i \neq j \neq k} b_{ij}^2 b_{ik} b_{jk} b_i b_j$	79.10	93.26	14.27
$S_{12} = \sum_{i \neq j \neq k} b_{ij}^2 b_{ik} b_{jk} b_j b_k$	19.45	15.81	0.394

TABLE II. Moments of the symmetric dipolar fluctuation spectral density associated with the ADRF autocorrelation function, Eq. (2.41), for a CaF<sub>2</sub> crystal, calculated from Eqs. (3.15) and (3.16).

Direction of $\vec{H}_0$	$M_2$ ( $10^9 \text{ sec}^{-2}$ )	$M_4$ ( $10^{18} \text{ sec}^{-4}$ )	$M_4/(M_2)^2$
[100]	1.011	9.034	8.8
[110]	0.544	1.962	6.6
[111]	0.305	0.550	5.9

for the cross-polarization spectra and transient oscillations.

To accomplish this program, for pure dipolar interactions between equivalent  $I$  spins, the expressions for the second and fourth moments of the  $C_\alpha(\tau)$  functions may be formulated in a compact way in terms of the lattice sums  $S_n$  defined in Table I. For the ADRF autocorrelation function, Eq. (2.41), we get (hereafter we drop the superscript zero)

$$M_2 = \frac{2I(I+1)}{27} \frac{S_1 S_2 - S_4}{S_1}, \quad (3.15)$$

$$\begin{aligned} M_4 = \frac{2I(I+1)}{243} \frac{1}{S_1} \{ \frac{1}{5} [16I(I+1) - 7] [S_1 S_3 - 2S_5] \\ + \frac{1}{3} I(I+1) [13S_7 - 16S_8 + 3S_9 - 8S_{10} + 16S_{11} - 8S_{12}] \}, \end{aligned} \quad (3.16)$$

and similarly for the SL case, from Eq. (2.40),

$$M_2 = P_2 (\cos \theta_I)^2 \frac{I(I+1)}{27} \frac{(5S_1 S_2 + 8S_4)}{S_1}, \quad (3.17)$$

$$\begin{aligned} M_4 = P_2 (\cos \theta_I)^4 \frac{I(I+1)}{243} \frac{1}{S_1} \{ \frac{1}{5} [101I(I+1) - \frac{49}{2}] S_1 S_3 \\ + \frac{1}{5} [176I(I+1) - 32] S_5 + \frac{1}{3} I(I+1) [77S_7 \\ + 88S_8 + 24S_9 + 8S_{10} + 38S_{11} + 8S_{12}] \}. \end{aligned} \quad (3.18)$$

These general expressions for the first two moments of our dipolar fluctuation spectral densities were evaluated for the case of the <sup>43</sup>Ca-<sup>19</sup>F system in the calcium fluoride crystal, using the values of the lattice sums given in Table I. The results are shown for ADRF and SL cases in Tables II and III. From these values it is evident that especially for

TABLE III. Moments of the symmetric dipolar fluctuation spectral density associated with the SL autocorrelation function, Eq. (2.40), for a CaF<sub>2</sub> crystal. The moments are computed from Eqs. (3.17) and (3.18) with  $\theta_I = \pi/2$ .

Direction of $\vec{H}_0$	$M_2$ ( $10^9 \text{ sec}^{-2}$ )	$M_4$ ( $10^{18} \text{ sec}^{-4}$ )	$M_4/(M_2)^2$
[100]	1.501	5.455	2.4
[110]	0.487	0.649	2.7
[111]	0.192	0.113	3.1

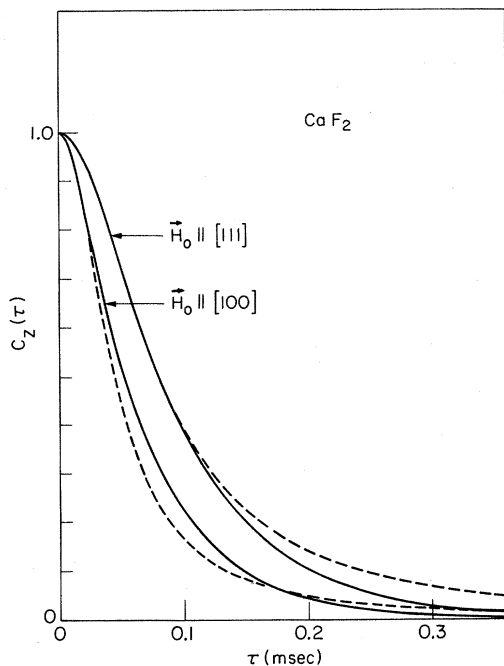


FIG. 2. Autocorrelation functions of the  $^{43}\text{Ca}$ - $^{19}\text{F}$  dipolar coupling for  $\text{CaF}_2$  with the  $^{19}\text{F}$  spins in the ADRF state (solid curves). The curves have been computed from the dipolar fluctuation spectrum, Eq. (3.13), based on a Gaussian memory function. For comparison Lorentzians  $(1 + \tau/\tau_c)^{-1}$  have been included (dashed curves) with the theoretical correlation times from Table IV.

$\vec{H}_0$  parallel to the [111] direction the dipolar fluctuation spectral density function is close to exponential [a pure exponential has  $M_4/(M_2)^2 = 6$ ] for the ADRF case and to a Gaussian [a pure Gaussian has  $M_4/(M_2)^2 = 3$ ] for the SL case, in the short-time region. From these values of moment ratio it also follows that the shape of  $J_x(\omega)$  for orientation [100] is more flat topped than a Gaussian. This flat-topped spectral density corresponds by Fourier transformation to an autocorrelation function which oscillates as it decays to zero. Also the shape of  $J_z(\omega)$  is changed for this orientation, the spectral density

TABLE IV. Correlation times  $\tau_c$  for the dipolar fluctuation autocorrelation functions  $(1 + \tau^2/\tau_c^2)^{-1}$  and  $\exp(-\tau^2/\tau_c^2)$  for a  $\text{CaF}_2$  crystal. The correlation time is taken to be  $\tau_c = (2/M_2)^{-1/2}$  with the  $M_2$  values from Tables II and III. The experimental values are taken from McArthur *et al.* (Ref. 5).

Direction of $\vec{H}_0$	$\tau_c$ ( $\mu\text{sec}$ )		
	ADRF condition	SL condition ( $\theta_I = \pi/2$ )	
	Present theory	Experimental values	
[100]	45	•••	37
[110]	61	$57 \pm 0.5$	64
[111]	81	$78 \pm 1; 80 \pm 1$	102

being narrowed in the low-frequency domain, as is a Lorentzian curve.

Using computed Fourier transformations from Eqs. (3.14), (3.13), and (2.39), a numerical representation for the dipolar fluctuation autocorrelation function is obtained. The functions  $C_Z(\tau)$  and  $C_X(\tau)$  are depicted in Figs. 2 and 3 together with pure Lorentzian and Gaussian shape functions, respectively. The parameters of the last curves are determined from Table IV. We note the Lorentzian and Gaussian characters of  $C_Z(\tau)$  and  $C_X(\tau)$  functions for small values of time. The SL dipolar fluctuation autocorrelation function manifests beat structure similar to FID, which is also plotted for comparison.<sup>35, 63</sup>

The knowledge of the dipolar fluctuation spectral density functions from Eq. (3.13) makes it trivial to compute the cross-polarization spectra. Figures 4(a) and 4(b) show the cross-polarization spectra,  $T_{IS}^{-1}$  vs  $\omega_{\text{ext},s}$ , evaluated from Eq. (2.39) and Table V with  $\theta_s = \pi/2$ . McArthur *et al.*<sup>5</sup> have measured such spectra in the ADRF case for [111] and [110] orientations, and these experimental data are also plotted. Our theoretical spectra, which have

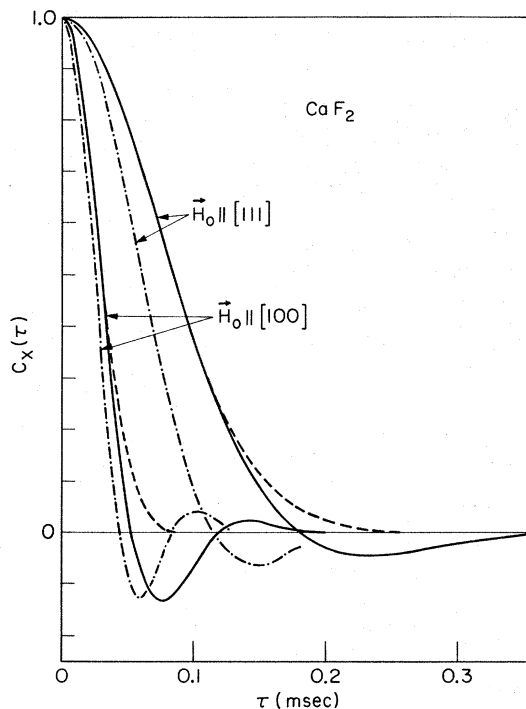


FIG. 3. Dipolar fluctuation autocorrelation functions for  $\text{CaF}_2$  with the abundant spin system in the SL condition (solid curves), derived from a Gaussian memory function. The dashed curves are the Gaussians,  $\exp(-\tau^2/\tau_c^2)$  with  $\tau_c$  from Table IV. Also included in this figure are the experimental  $^{19}\text{F}$ -free-induction decays (Ref. 63) (dot-dashed lines), twice extended in time for the same orientations of the crystal.

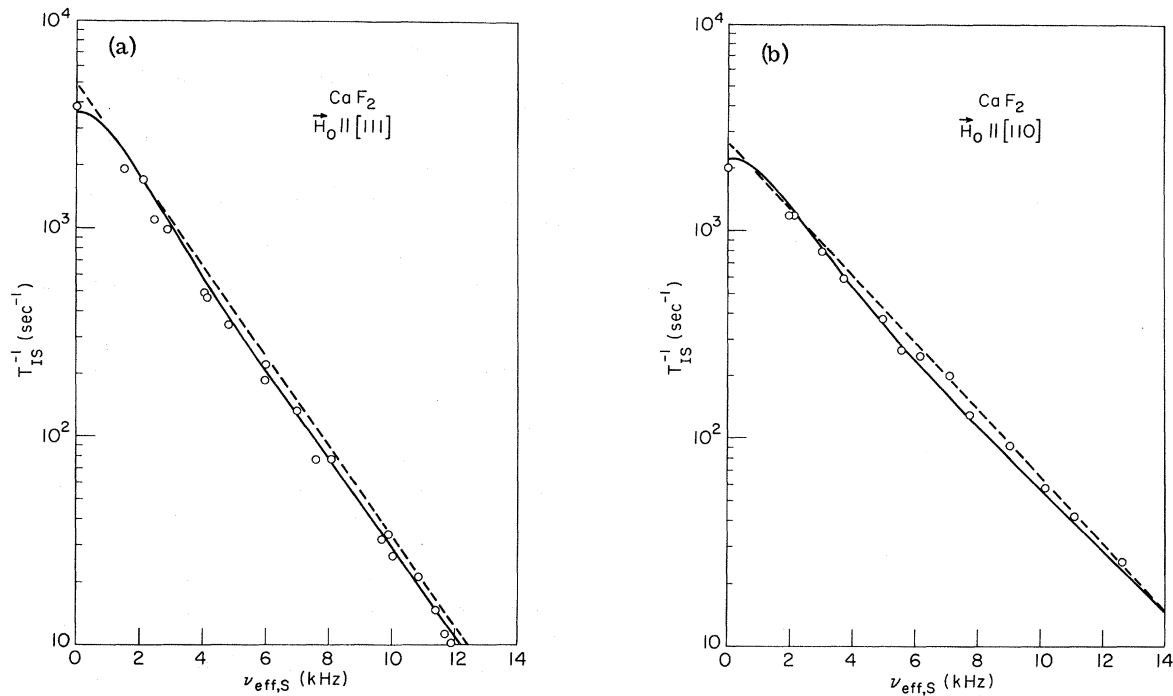


FIG. 4. Cross-polarization spectra under ADRF conditions for  $^{43}\text{Ca}$ - $^{19}\text{F}$  in a  $\text{CaF}_2$  crystal for two different orientations: (a)  $H_0 \parallel [111]$ ; (b)  $H_0 \parallel [110]$ . Circles are experimental points of McArthur *et al.* (Ref. 5), and the dashed line is their fit to an exponential spectrum. The solid line is calculated from the present theory.

no adjustable parameters of any kind, agree with their measurements in every case within experimental error. Similar agreement is also evident from the off-resonance dependence of cross-relaxation spectra shown in Figs. 5(a) and 5(b).

From Figs. 4(a) and 4(b) it is seen that the data points and our theoretical spectra do not form a straight line but are slightly concave upward. This curvature, which becomes more evident for the [110] orientation, seems to be an intrinsic feature of the spectrum and is not related to the spin-diffusion effects or high-order processes.<sup>5</sup> Our theory is valid only for large values of effective field applied to the  $S$  spins compared with their local field, and consequently the functional form of theoretical cross-relaxation spectra must break down as  $\omega_{\text{eff},S} \rightarrow 0$ . At the same time, because autocorrelation functions are well described by the memory-function approach for short times, we expect a good agreement with experimental data only in the high-effective-frequency domains.

The cross-polarization spectra for the SL case can be calculated by the same procedure used in the ADRF case. The dependence of  $T_{IS}^{-1}$  on the difference between the effective frequencies of  $S$  and  $I$  spins in their tilted rotating frames is shown in Fig. 6 for a  $\text{CaF}_2$  crystal. We note a completely different behavior compared with the ADRF case, with generally larger values of  $T_{IS}$ . As one goes

from  $\vec{H}_0$  along [111] to [110] and [100], the cross-relaxation spectrum becomes less and less nearly exponential for the ADRF case and less and less nearly Gaussian for the SL case.

The short-time behavior of coupled  $I$ - and  $S$ -spin systems in a double-resonance experiment can be analyzed from Eqs. (2.44) and (2.45), Table V, and the Fourier transformation of Eq. (3.13). A comparison between the theoretical results and experimental data<sup>5</sup> for transient oscillations in the rotating frame for the  $^{43}\text{Ca}$ - $^{19}\text{F}$  system is presented in Figs. 7(a) and 7(b). From these figures it again is seen that our dipolar fluctuation autocorrelation function  $C_z(\tau)$  is very well approximated by a Lorentzian only for small values of time, and an improvement in its functional shape for long time is needed in order to describe all the experimentally observed oscillations. The slope of the dashed line, which characterizes the beginning of the expo-

TABLE V. Values of Van-Vleck second moment of the  $S$  magnetic resonance line,  $M_{2,SI}$ , and local field of  $I$ -spins in the rotating frame,  $H'_{LI}$  for the  $\text{CaF}_2$  crystal.

Direction of $\vec{H}_0$	$M_{2,SI}$ ( $10^7 \text{ sec}^{-2}$ )	$H'_{LI}$ (G <sup>2</sup> )
[100]	0.21	4.24
[110]	2.78	1.61
[111]	3.64	0.73

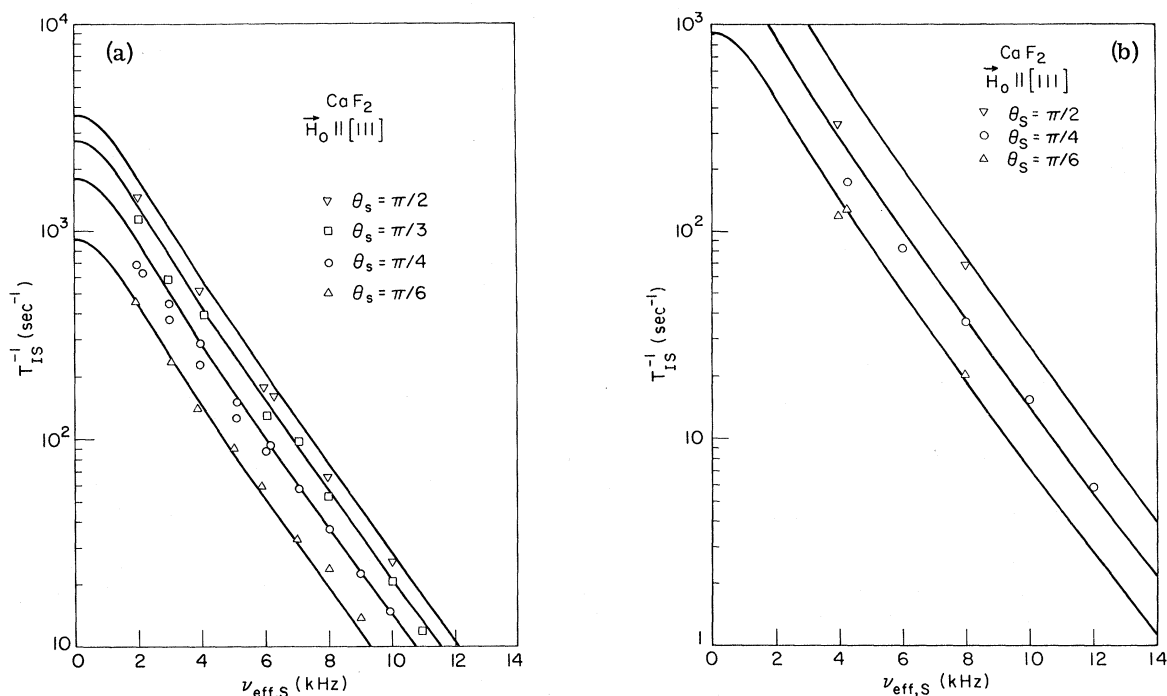


FIG. 5. "High-resolution effect" on cross-polarization spectra for  $^{43}\text{Ca}$ - $^{19}\text{F}$  in a  $\text{CaF}_2$  crystal measured by (a) indirect pulsed double-resonance and (b) rotary saturation double resonance methods (Ref. 5). The  $\sin^2\theta_s$  dependence of our theoretical cross-relaxation spectra (solid lines) well reproduces the experimental data.

nential cross-relaxation process, was found to be very sensitive to the value of the autocorrelation function. Also, it is clear from Fig. 7(b) that in order to obtain a better agreement between the theoretical results and experimental data the theory has to be extended to the low-effective-field condition for dilute spins. In this case the  $I$ - $S$  coupling cannot be considered any longer as a small perturbation, and the general theory of Sec. II B should be applied.

The enhanced transient oscillation effect which appears as a function of the crystal orientation for  $\text{CaF}_2$  was also calculated for the ADRF case and is shown in Fig. 8. We see that for the  $[100]$  orientation the step-plus-oscillation form of transient behavior is reduced compared with the  $[111]$  orientation because of the smaller values of Van Vleck cross-coupling second moment and autocorrelation time (see Table IV), which makes the dipolar fluctuation autocorrelation function decay more rapidly. This explains the experimental difficulty in measurement of transient oscillations for orientations different from  $[111]$ .<sup>5</sup> The enhanced transient oscillation for  $[111]$  orientation is a result of a reduced dipolar coupling between abundant spins which makes the coherent exchange of energy between  $I$ - and  $S$ -spin systems to be more like that for an  $I$ - $S$  spin pair.<sup>3, 57, 64</sup>

Similar computations can be performed for the

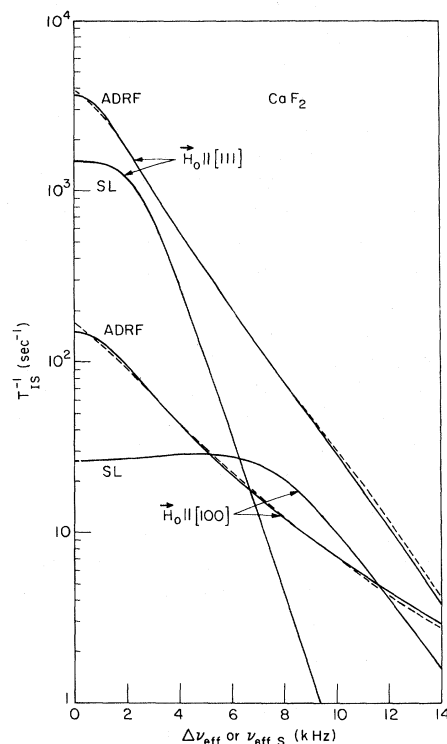


FIG. 6. Theoretical cross-polarization spectra for SL and ADRF cases and for different orientations of the  $\text{CaF}_2$  crystal. The dashed curves are calculated using an information-theory approach from Eq. (3.19) and Table VI.

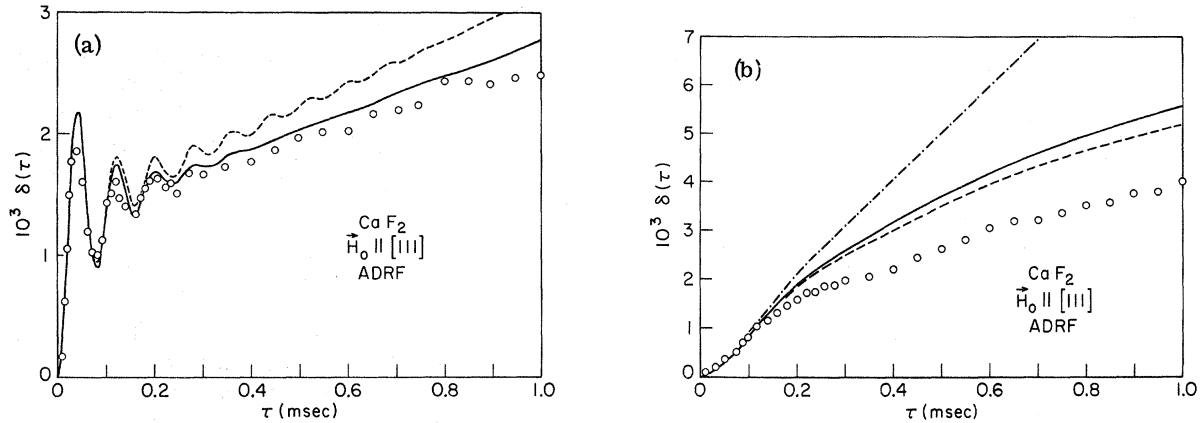


FIG. 7. Transient oscillations in the rotating frame for the  $^{43}\text{Ca}$ - $^{19}\text{F}$  system in a  $\text{CaF}_2$  crystal for the ADRF condition. The function  $\delta(\tau)$  is the fractional decrease in the  $I$ -spin signal after a mixing pulse and was calculated from the theoretical results of Ref. 5 with our autocorrelation function and numerical values from Table V (solid curves). (a) The experimental data points are from Ref. 5 with  $\nu_{\text{eff},S} = 12.6$  KHz. The dashed curve has been calculated using a Lorentzian autocorrelation function with  $\tau_c = 77$   $\mu\text{sec}$  (Ref. 5). (b) Same as (a) except with  $\nu_{\text{eff},S} = 2.43$  KHz and the correction due to the cross-relaxation process included (see Ref. 5). Also shown is the  $\delta(\tau)$  function (dot-dashed line) calculated from our autocorrelation function without the exponential correction.

SL condition from Eq. (2.44). Figure 9 shows these results in the matched and mismatched Hartmann-Hahn conditions.<sup>3</sup> We remark that, because the amplitude of the dilute spin magnetization  $M_S(\tau)$  in the short-time domain is proportional to the inverse spin temperature of abundant spins, the signals which are measured in the ADRF case are bigger than those in the SL case.

The short-time behavior of two spin systems in interaction for a many-body  $I$  system with strong interactions between the components can be understood as a limiting case of an  $I$ - $S$  spin pair. In the last case, for the matched Hartmann-Hahn SL condition, a coherent exchange of energy between  $I$  and  $S$  spins takes place with frequency  $\frac{1}{2}b_{im}$ .<sup>57,64</sup> As additional  $I$  spins are brought into interaction with the  $S$  spin the coherence is damped and a degenerate transient oscillation like that plotted in Fig. 9 occurs. When the Hartmann-Hahn condition is violated the oscillation frequency for a spin pair becomes  $(\Delta\omega_{\text{eff}}^2 + \frac{1}{4}b_{im}^2)^{1/2}$  and the step-plus-oscillation begins to be evident (see Fig. 9) in the many-body limit. If  $\omega_{\text{eff},I} \rightarrow 0$ , as in the ADRF condition, and  $\omega_{\text{eff},S}$  is large compared with the width of the low-resolution  $S$ -spin resonance line, the oscillation frequency depends only on  $\omega_{\text{eff},S}$  as Figs. 7 and 8 prove.

#### B. Information-theory approach

The functional form of a spectral density function can be efficiently approximated by using only its moments in the framework of information theory<sup>37,38</sup> and error-bound methods.<sup>65-67</sup> We shall deal here only with the former approach in its nonclassical version,<sup>38</sup> but the error-bound method works equal-

ly well.

In the high-effective-field condition, which corresponds to the SL case, the actual distribution of frequencies for the spectral density function  $J_x(\Delta\omega_{\text{eff}})$  is to a good approximation symmetric around  $\Delta\omega_{\text{eff}} = 0$ . The odd moments for this distribution of frequencies can be considered equal to zero. The even moments are given in Table III for a  $\text{CaF}_2$  crystal in a double-resonance experiment in

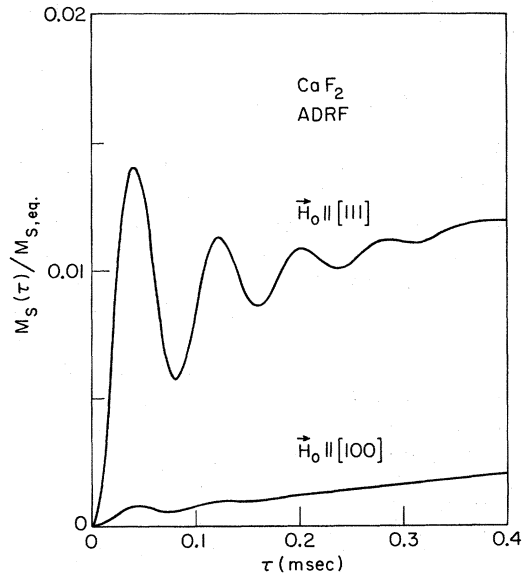


FIG. 8. Transient oscillations in the rotating frame of normalized  $S$ -spin magnetization calculated from Eq. (2.45) and Table V for a  $\text{CaF}_2$  crystal. ADRF conditions are assumed with  $\nu_{\text{eff},S} = 12.6$  KHz as in Fig. 7.

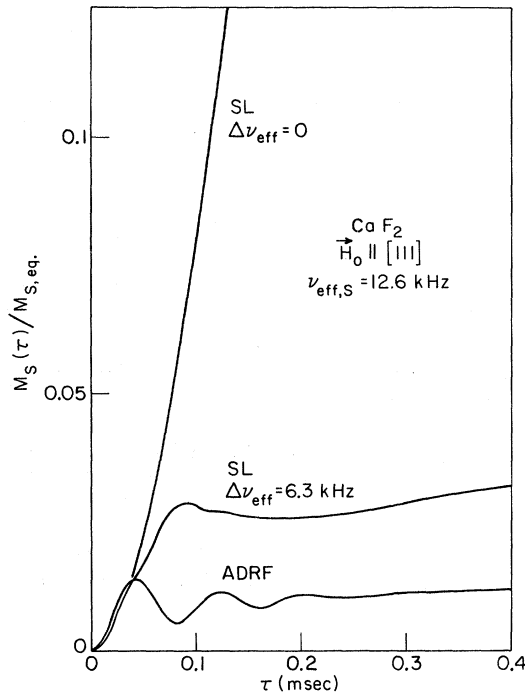


FIG. 9. Short-time behavior of normalized S-spin magnetization calculated from Eq. (2.44) and Table V for a CaF<sub>2</sub> crystal, in matched ( $\Delta\nu_{\text{eff}}=0$ ) and mismatched ( $\Delta\nu_{\text{eff}}=6.3$  KHz) Hartmann-Hahn SL condition. The transient oscillations in the rotating frame for the ADRF case with  $\nu_{\text{eff},S}=12.6$  KHz is also represented (see Fig. 8) for comparison.

which  $I$  spins are irradiated exactly at resonance, ( $\theta_I = \pi/2$ ). We remark here that apparently the ratio  $M_4/(M_2)^2$  is from Eqs. (3.17) and (3.18) independent of  $\theta_I$ . In reality, as  $\theta_I$  approaches the magic value of  $\theta_m = \cos^{-1}(1/\sqrt{3})$ , the expression (2.40) for the dipolar fluctuation autocorrelation function is no longer valid and so neither is the definition of the moments. Comparing our values of the moment ratios given in Table III with the corresponding values for CaF<sub>2</sub>, we see from the information theory of Powles and Cazazza<sup>37,38</sup> that the most probable spectral density shape which we expect is a Gaussian, as indeed was proved by direct

computation in Sec. III A.

In order to analyze how surprising the spectral density exponential shape obtained experimentally<sup>5</sup> is in the low-field case for the CaF<sub>2</sub> single crystal, we use the nonclassical information theory<sup>38</sup> from which the most probable cross-relaxation spectrum is in our case given by

$$T_{IS}^{-1}(\omega) = \frac{A}{\exp(\alpha_0 + \alpha_1\omega + \alpha_2\omega^2 + \alpha_3\omega^3) - 1}, \quad (3.19)$$

where  $A$  and  $\alpha_i$  ( $i=1,3$ ) are related to the finite information available, the moments  $M_n$  ( $n=0,4$ ) of asymmetric spectral density function. Two difficulties appear if a concrete evaluation of the most probable  $T_{IS}^{-1}(\omega)$  spectrum is intended. The first is related to the theoretical evaluation of odd moments, which can be done only if the dipolar fluctuation autocorrelation function  $C_Z(\tau)$ , Eq. (2.41), is known. Thus  $M_1$  and  $M_3$  were estimated from experimental cross-relaxation spectra, Fig. 4(a), and from our theoretical cross-relaxation spectra, Fig. 6, for [111] and [100] orientations, respectively. Also it is difficult to obtain analytical relations for  $A$  and  $\alpha_i$  in terms of  $M_n$ . This problem was circumvented by a computer searching procedure in which a unique set of  $A$  and  $\alpha_i$  parameters were fitted to the moment value (see Table VI). The plot of Eq. (3.19) with the parameters from Table VI is given in Fig. 6. In spite of the approximations made in the evaluation of cross-polarization spectra, [Eq. (3.19)], good agreement exists with the Gaussian memory-function approach and so with the experimental results.<sup>5</sup> Therefore, at least for the calcium fluoride structure, the most probable cross-polarization spectrum which we expect in ADRF double-resonance experiments is close to an exponential. The functional form of this spectrum seems to be insensitive to the sample structure, as measurements of the cross-relaxation spectra of <sup>13</sup>C nuclei in some organic solids shows.<sup>12,13</sup>

### C. General remarks

We were originally stimulated to study this problem in part by the remarkable adherence of the ex-

TABLE VI. Parameters in the cross-polarization spectrum,  $T_{IS}^{-1}(\omega) = A[\exp(\sum_i \alpha_i \omega^i) - 1]^{-1}$  ( $i=0,3$ ). The ADRF case is considered for a CaF<sub>2</sub> crystal. The moments  $M_1$  and  $M_3$  are estimated from the experimental data [Fig. 4 (b)] or the theoretical spectrum (Fig. 6) for [111] and [100] orientations, respectively.  $M_2$  and  $M_4$  are from Table II. The numbers in the brackets are the moment ratios obtained with  $A$ ,  $\alpha_0$ ,  $\alpha_1$ ,  $\alpha_2$ , and  $\alpha_3$  values from Eq. (3.19) in the computer searching procedure.

Direction of $\vec{H}_0$	$A$	$10^3 \alpha_0$	$\alpha_1$ ( $10^{-7}$ sec)	$\alpha_2$ ( $10^{-12}$ sec <sup>2</sup> )	$\alpha_3$ ( $10^{-15}$ sec <sup>3</sup> )	$M_2/(M_1)^2$	$M_3/(M_1)^3$	$M_4/(M_1)^4$
[100]	0.69	4	2.2	1.6	0.28	2.28 (2.28)	8.68 (8.68)	46.0 (46.0)
[111]	57	15	6.9	0.12	3.9	1.95 (1.95)	5.72 (5.72)	22.3 (22.1)

perimental dipolar fluctuation spectra of MacArthur *et al.* to an exponential form; any such simple behavior must be underlain by a single physical explanation. Unfortunately, the approaches we have taken (memory functions, information theory) necessarily sacrifice "understanding" for tractability. However, the results we obtain make it appear that the exponential spectrum is only an approximate accident characteristic of certain special cases and not a general phenomenon understandable on the basis of a simple picture. Therefore it is not possible to say, any more than in other aspects of line-shape theory, what definitive property of the spin system, governed by its lattice structure, is manifested by the measured spectral character.

#### IV. THREE SPIN SPECIES

The double-resonance experiments can also be performed in situations in which a third abundant spin species  $X$  is present, together with  $I$ - and  $S$ -spin systems which are prepared and put in contact by radio-frequency irradiations close to their Larmor frequencies. Using the general theory developed in Sec. II, a quantitative study of the effects of the third spin system on  $I$ - $S$  spin dynamics is possible. Here we limit ourselves to a qualitative description in the high and low effective fields which are cases of experimental interest. Generally the presence of the  $X$ -spin system has three main effects: (a) The first is related to the change in the heat capacity of the  $I$ -spin system through changes in the local field. (b) The second effect of the  $X$  spins is to open an additional cross-relaxation path via the  $S$ - $X$  interaction. (c) The dipolar fluctuations in the  $X$ -spin system will affect the dipolar fluctuation spectrum of  $I$  spins through  $I$ - $X$  coupling.

To analyze the importance of these effects let us consider first the SL case with high effective fields compared with the width of the  $I$ - and  $S$ -spin resonance lines. In this case the (a) and (b) effects are reduced and the  $I$ - $S$  dynamics are less affected by the presence of the third spin system if we neglect its coupling with the lattice. This can be seen, for instance, by evaluating cross-polarization spectra from Eq. (2.36) in the hypothesis of a pure  $X$ -spin Zeeman Hamiltonian and small  $I$ - $S$  and  $X$ - $S$  dipolar interactions between the spins. The cross-polarization spectrum has the form

$$T_{IS}^{-1} = \frac{1}{2} \sin^2 \theta_S \sin^2 \theta_I M_{2,SI} J_X^I(\Delta\omega_{\text{eff}}) + \sin^2 \theta_S M_{2,SX} J_Z^X(\omega_{\text{eff}}, S), \quad (4.1)$$

where  $M_{2,SI}$  and  $M_{2,SX}$  are the Van Vleck<sup>2</sup> second moments of the  $S$  magnetic-resonance line determined by  $S$ - $I$  and  $S$ - $X$  dipolar interactions, respectively. The  $J_\alpha^I(\omega)$  ( $\alpha = X, Z$ ) spectral density functions are defined as in Eqs. (2.39), (2.40), and

(2.41), but with  $\mathcal{H}_{II}^0$  replaced by the Hamiltonian  $\mathcal{H}_{II}^0 + \mathcal{H}_{IX}^0 + \mathcal{H}_{XX}^0$ . The same Hamiltonian characterizes the spectral density function  $J_Z^X(\omega)$ , which has the same functional form as  $J_Z^I(\omega)$  but with the  $\sum_i b_i I_{iz}$  operator replaced with the corresponding operator for the  $X$ -spin system. As in to the case of free-induction decay in a system with different spin species,<sup>29,34</sup> we do not expect drastic changes in functional form of cross-relaxation spectra compared with the  $I$ - $S$  case. In conclusion, only the (c) effect is dominant compared with (a) and (b) in the SL case. This effect will have a large influence on the  $I$ - $S$  spin dynamics, for instance, in the case of an  $S$ - $X$  spin pair. A direct evaluation of short-time behavior using Eq. (2.29) also shows a small  $X$ -spin effect mainly determined by its high spin temperature compared with the  $I$ -spin-system temperature.

Completely different  $I$ - $S$  spin dynamics take place in general for the ADRF case in which the presence of  $X$  spins has a large effect. Now the cross-polarization spectrum has the following form:

$$T_{IS}^{-1} = \sin^2 \theta_S M_{2,SI} J_Z^I(\omega_{\text{eff}}, S) + \sin^2 \theta_S M_{2,SX} J_Z^X(\omega_{\text{eff}}, S). \quad (4.2)$$

Similarly for transient oscillations in the rotation frame, we obtain

$$M_S(\tau)/M_{S,\infty} = \sin^2 \theta_S (1 + \epsilon) \int_0^\tau dt_1 \int_0^{t_1} dt_2 \times \cos(\omega_{\text{eff}, S} t_2) [M_{2,SI} C_Z^I(t_2) + M_{2,SX} C_Z^X(t_2)], \quad (4.3)$$

where  $\epsilon$  is the ratio of the  $S$  to  $I+X$  heat capacities. In derivation of the above equations from the results of Sec. II it had been considered that the  $I$ - and  $X$ -spin reservoirs are in thermodynamic equilibrium before the contact with the dilute spin system. The cross-polarization spectrum, Eq. (4.2), consists now of a weighted sum of two spectral density functions. In the short-time domain the  $S$ -spin magnetization oscillates with the frequency  $\omega_{\text{eff}, S}$ , but this transient behavior has a step value and a damping dependent on both  $I$  and  $X$  dipolar fluctuation autocorrelation functions.

In order to analyze how the functional form of spectral density functions  $J_Z^I$  and  $J_Z^X$  changes in the presence of the third spin, we remark that the second moments of these distributions are not affected by the  $\mathcal{H}_{IX}^0 + \mathcal{H}_{XX}^0$  and  $\mathcal{H}_{IX}^0 + \mathcal{H}_{II}^0$  Hamiltonians, respectively. Because that is not true for the fourth moment, we expect a change in the ratio  $M_X/(M_Z)^2$  and so in the functional form of the spectral density. If  $\gamma_I \gg \gamma_X$  the shape of  $J_Z^I(\omega)$  remains close to an exponential, but  $J_Z^X(\omega)$  will approach a Lorentzian form. An opposite situation occurs when  $\gamma_I \ll \gamma_X$ . This last case corresponds to the experi-

ment of Lang and Moran<sup>11</sup> in LiF with  $I = {}^7\text{Li}$ ,  $S = {}^6\text{Li}$ , and  $X = {}^{19}\text{F}$ . From this qualitative discussion we cannot confirm or deny the experimental Lorentzian cross-relaxation spectrum obtained for LiF under ADRF conditions. Only a concrete evaluation of Eq. (4.2) for this system will show if our theoretical cross-relaxation spectrum is a good approximation in this case. The second-order perturbation theory which works very well for  $\text{CaF}_2$  does not seem to be any longer valid in the LiF case because of the relatively large value of magnetogyric ratio  $\gamma_S/\gamma_I$  for the  ${}^6\text{Li}$ - ${}^7\text{Li}$  spin system. Consequently, a higher-order perturbation theory has to be applied in order to describe the cross-polarization dynamics.

### V. EXPERIMENTAL CONSEQUENCES

One of our goals in this work was to understand the factors which govern the sensitivity with which the NMR spectra of rare spins, polarized by contact with abundant spins, can be detected. From the view point of signal-detection theory, this sensitivity is governed by the magnetization  $M_S$  acquired in a typical thermal contact and by the total rate at which this acquisition can be repeated. That is, one can define an experimental quality factor  $Q = M_S^2/T_R$ , where  $T_R$  is the time between thermal mixing (and measuring) events. In general  $M_S$  and  $T_R$  represent suitable averages over an epoch which is capable of exact and periodic repetition.

First consider the conditions placed on  $M_S$  by thermodynamics for a single thermal contact, before which the  $I$  spins have their Curie magnetization at the lattice temperature  $T_L$ ;  $M_{0I} = C_I H_0/T_L$ , and the  $S$  spins are completely disordered. The  $I$  spins are first supposed to be demagnetized isentropically to a field  $H_I$ , which will be the effective field  $[H_I^2 + (H_0 - \omega_I/\gamma_I)^2]^{1/2}$  in the case of strong spin locking or the (truncated) local field  $H'_{LI}$  in the case of ADRF. Thermal mixing then occurs with an effective field  $H_{\text{eff},S}$  applied to the rare spins, the total spin energy being conserved. At equilibrium one easily finds

$$M_S/M_{0S} = (\gamma_I/\gamma_S)\eta/(1 + \epsilon\eta^2), \quad (5.1)$$

where  $\epsilon = N_S S(S+1)/N_I I(I+1)$  and  $\eta = \gamma_S H_{\text{eff},S}/\gamma_I H_I$ .

If one's goal is to maximize this quantity, without regard for the time required to reach equilibrium or other factors, one chooses  $\eta^{(0)} = (\epsilon)^{-1/2}$ , leading to

$$(M_S/M_{0S})_{\text{max}} = \frac{1}{2}(\gamma_I/\gamma_S)\epsilon^{-1/2}. \quad (5.2)$$

A situation of considerably more widespread practical interest than the  ${}^{43}\text{Ca}$ - ${}^{19}\text{F}$  case described above is the one in which  $I = {}^1\text{H}$  and  $S = {}^{13}\text{C}$  at natural isotopic abundance in a typical organic solid, for which  $\epsilon^{-1} \sim 150$ . For this case the maximum trans-

fer is for  $\eta \sim 12$  and gives  $(M_S/M_{0S})_{\text{max}} \sim 24$ .

It is the large value of  $\eta$  for which maximum  $M_S$  is achieved that requires one to examine the role of the time  $T_{IS}$  characterizing the approach to equilibrium. Figure 6 illustrates the strong dependence of  $T_{IS}$  on  $\eta$  and the fact that this dependence is quite different under SL and ADRF conditions. For sufficiently large values of  $\eta$  it would appear in general that ADRF is to be preferred on the basis of rate of equilibrium. However, such rates may in either case become so slow in practice that limits are set by factors not yet considered, in particular spin-lattice relaxation of the  $I$  spins which competes with the cross-polarization process. Suppose we consider a single thermal mixing, as above, but adjust  $\eta$  so that  $T_{IS} = T_{1DI}$  in the ADRF case or  $T_{IS} = T_{1\rho I}$  in the SL case.<sup>68</sup> For simplicity we represent the cross-polarization spectra as exponential in the ADRF case and Gaussian for the SL case, as described above. With a little manipulation from Eqs. (2.38) and (2.42), one finds

$$\left(\frac{M_S}{M_{0S}}\right)_{\text{ADRF}} = \frac{\gamma_I}{\gamma_S} \frac{\eta_1}{1 + \epsilon\eta_1^2}, \quad (5.3)$$

$$\eta_1 = (\tau_{c1}\omega'_{LI})^{-1} \ln(\pi M_{2,SI}\tau_{c1}T_{1DI}/2)$$

and

$$\left(\frac{M_S}{M_{0S}}\right)_{\text{SL}} = \frac{\gamma_I}{\gamma_S} \frac{\eta_2}{1 + \epsilon\eta_2^2}, \quad (5.4)$$

$$\eta_2 = 1 + 2(\tau_{c2}\omega_{II})^{-1} [\ln(\sqrt{\pi} M_{2,SI}\tau_{c2}T_{1\rho I}/2)]^{1/2}.$$

For simplicity the spin-lattice relaxation has been treated as though  $M_I$  were unaffected by it for a time  $T_{IS}$  and then disappeared altogether.

A direct comparison of the efficiencies of SL and ADRF procedures requires a knowledge of the appropriate correlation times and spin-lattice relaxation times. One knows that  $T_{1DI} < T_{1\rho I}$ , but these times are often of the same order of magnitude. Then for the  ${}^{43}\text{Ca}$ - ${}^{19}\text{F}$  system, for instance, in the [111] orientation of the  $\text{CaF}_2$  crystal, from Tables IV and V and for  $H_{1I} = 5$  G with  $T_{1DI} \sim T_{1\rho I}$ , we get, from Eqs. (5.3) and (5.4),  $(M_S/M_{0S})_{\text{ADRF}}/(M_S/M_{0S})_{\text{SL}} \sim 15$ . Even if  $T_{1DI}$  is smaller than  $T_{1\rho I}$  in practice the mismatch ADRF experiment is preferred because of the presence of only one rf field in the probe. This fact, together with exponential character of cross-polarization spectrum, leads in general to a gain in sensitivity of the mismatch ADRF experiment compared with the mismatch SL case.

But is a single thermal mixing during the spin-lattice lifetime of the  $I$  spins a tactically optimal procedure? One could in principle compare this procedure with one in which  $n$  thermal contacts are made in the same total time, taking into account the buildup of noise energy proportional to  $n$  in the

process of co-addition of  $n$  free-induction decays. Such a comparison requires consideration of a number of sample-dependent parameters and is perhaps unprofitable. Calculations based on the  $\text{CaF}_2$  situation support a slight advantage in multiple over single contacts.

We can also compare a process of *isentropic* transfer of polarization from the abundant spins prepared in an ADRF condition to the dilute spins with the irreversible transfer performed in a mismatch ADRF experiment in the same final effective field. In the first case the order is, at the beginning of the experiment, transferred from the Zeeman reservoir of  $I$  spins to the dipolar reservoir represented by the total  $I$  and  $S$  dipolar Hamiltonian. As  $I$  spins are demagnetized they become cold, but the  $S$ -spin system is still at a very high effective spin temperature and at some value of  $H_I$  thermal mixing must begin between  $I$  and  $S$  at different temperatures. This cannot be isentropic. Of course, the "irreversibility" is small because  $C_S \ll C_I$ . At the end of this process the  $I$  and  $S$  spins are both ordered in their local fields and this order can be isentropically (and thus reversibly) transferred to the Zeeman reservoir of the rare spins by increasing the intensity of the  $S$  rf field, for instance, from zero to a final value  $\omega_{1S}/\gamma_S$  in such a manner that the local isentropic condition,  $d\omega_{1S}/dt \ll \omega_{1S}/T_{IS}(\omega_{1S})$ , is satisfied.

Let us suppose that a *complete* transfer is indeed possible. The conservation of entropy requires that

$$S_{\text{before}} = S_{\text{after}} \quad (5.5)$$

where we assume that  $S_{\text{before}}$  reflects  $I$ -spin order only, and  $S_{\text{after}}$  has *all* order transferred to the  $S$  spins. Then we find

$$(M_S/M_{0S})_{\text{it}} = (\gamma_I/\gamma_S)\epsilon^{-1/2} \quad (5.6)$$

From Eqs. (5.2) and (5.6) we can see that if only thermodynamic considerations are involved the isentropic transfer of order is better than optimum thermal mixing by a factor of 2. We note that for

$S_{\text{after}}(I)$  to be neglected compared to  $S_{\text{after}}(S)$  it is required that  $C_S H_{1S}^2/T_S^2 \gg C_I H_I^2/T_I^2$ , i. e.,  $\eta \gg \epsilon^{-1/2}$ . For the  $^{13}\text{C}$ - $^1\text{H}$  system in most organic compounds,  $\epsilon \approx \frac{1}{150}$ , and consequently  $\eta \gg 12$ , which is a more severe restriction than for optimum thermal mixing.

If a partial isentropic transfer of order is performed in a field  $\omega_{1S} = \eta\omega'_{LI}$ , from the conservation of the entropy principle we have

$$\left(\frac{M_S}{M_{0S}}\right)_{\text{it}} = \frac{\gamma_I}{\gamma_S} \frac{\eta}{(1 + \epsilon\eta^2)^{1/2}} \quad (5.7)$$

From Eq. (5.7) it follows that an isentropic transfer of polarization is now better than an optimum thermal mixing ( $\eta^{(0)} = 1/\sqrt{\epsilon}$ ) by a factor  $\sqrt{2}$ , for the same final value of the mismatch parameter  $\eta$ . But the interval of time in which these processes take place has to be taken into account. Thermal mixing requires a time  $T_{IS}(\eta^{(0)}\omega'_{LI})$ . To reach the same value of effective field  $\eta^{(0)}\omega'_{LI}$  the isentropic transfer of polarization requires a time  $T_{\text{it}} \gg T_{IS}(\eta^{(0)}\omega'_{LI})$ ; so the gain of  $\sqrt{2}$  is illusory. We have to consider also the fact that the ratio  $T_{\text{it}}/T_{1DI}$ , which has to be of the order of unity to make the experiment feasible, is increasing approximately exponentially with the value of the effective magnetic field applied to  $S$  spins. Consequently, it follows that the quasi-isentropic transfer of polarization is in general less efficient than the mismatched ADRF thermal mixing experiment. We note that it is possible to increase the value of the mismatch parameter and at the same time to reduce the rf power dissipated in the probe by using an *off-resonance* isentropic increase in the  $S$  effective-field. This is not so effective in practice because of the more rapid increase in the  $T_{\text{it}}/T_{1DI}$  parameter compared with on-resonance conditions.

#### ACKNOWLEDGMENTS

One of the authors (D. E. D.) is grateful for an International Atomic Energy (Vienna) fellowship held during the course of this work.

\*Supported in part by the National Science Foundation and in part by the National Institutes of Health.

†International Atomic Energy Agency Fellow, on leave from the Institute of Atomic Physics, Bucharest, Romania.

‡Permanent address: Institute of Chemistry, University of Uppsala, Uppsala, Sweden.

<sup>1</sup>F. Bloch, Phys. Rev. **70**, 460 (1946).

<sup>2</sup>J. H. Van Vleck, Phys. Rev. **74**, 1168 (1948).

<sup>3</sup>S. R. Hartmann and E. L. Hahn, Phys. Rev. **128**, 2042 (1962).

<sup>4</sup>F. M. Lurie and C. P. Slichter, Phys. Rev. **133**, A 1108 (1964).

<sup>5</sup>D. A. McArthur, E. L. Hahn, and R. E. Walstedt, Phys. Rev. **188**, 609 (1969).

<sup>6</sup>H. E. Bleich and A. G. Redfield, J. Chem. Phys. **55**, 540 (1971).

<sup>7</sup>P. K. Grannell, P. Mansfield, and M. A. B. Whitaker, Phys. Rev. B **8**, 4149 (1973).

<sup>8</sup>A. Pines, M. G. Gibby, and J. S. Waugh, J. Chem. Phys. **59**, 569 (1973).

<sup>9</sup>D. Demco, S. Kaplan, S. Pausak and J. S. Waugh, Chem. Phys. Lett. (to be published).

<sup>10</sup>I. Solomon, C. R. Acad. Sci. **248**, 92 (1959).

<sup>11</sup>D. V. Lang and P. R. Moran, Phys. Rev. B **1**, 53 (1970).

<sup>12</sup>J. Urbina (private communication).

<sup>13</sup>A. Pines and T. W. Shattuck, J. Chem. Phys. **61**, 1255 (1974).

<sup>14</sup>M. Goldman, *Spin Temperature and Nuclear Magnetic*

- Resonance in Solids* (Oxford U. P., London, 1970).
- <sup>15</sup>B. N. Provotorov, Zh. Eksp. Teor. Fiz. 41, 1582 (1961) [Soviet Phys.-JETP, 14, 1126 (1962)].
- <sup>16</sup>B. N. Provotorov, Zh. Eksp. Teor. Fiz. 42, 882 (1962) [Soviet Phys.-JETP, 15, 611 (1962)].
- <sup>17</sup>K. Kawasaki, Prog. Theor. Phys. 39, 285 (1968).
- <sup>18</sup>P. Résibois and M. DeLenner, Phys. Rev. 152, 305 (1966).
- <sup>19</sup>M. DeLenner and P. Résibois, Phys. Rev. 152, 318 (1966).
- <sup>20</sup>J. A. Tjon, Phys. Rev. 143, 259 (1966).
- <sup>21</sup>P. Borkmans and D. Walgraef, Phys. Rev. 167, 282 (1968).
- <sup>22</sup>F. Lado, J. D. Memory, and G. W. Parker, Phys. Rev. B 4, 1406 (1971).
- <sup>23</sup>G. F. Reiter, Phys. Rev. B 5, 222 (1972).
- <sup>24</sup>F. C. Barreto and G. F. Reiter, Phys. Rev. B 6, 2555 (1972).
- <sup>25</sup>G. F. Reiter, Phys. Rev. B 7, 3325 (1973).
- <sup>26</sup>W. A. B. Evens and J. G. Powles, Phys. Lett. A 24, 218 (1968).
- <sup>27</sup>M. Lee, D. Tse, W. I. Goldberg, and I. J. Lowe, Phys. Rev. 158, 246 (1967).
- <sup>28</sup>D. Demco, Phys. Lett. A 27, 702 (1968).
- <sup>29</sup>R. E. Fornes, G. W. Parker, and J. D. Memory, Phys. Rev. B 1, 4228 (1970).
- <sup>30</sup>H. Mori and K. Kawasaki, Prog. Theor. Phys. 27, 529 (1962).
- <sup>31</sup>H. S. Bennett and P. C. Martin, Phys. Rev. 138, A 608 (1965).
- <sup>32</sup>P. Mansfield, Phys. Rev. 151, 199 (1966).
- <sup>33</sup>G. W. Parker, Phys. Rev. B 2, 2453 (1970).
- <sup>34</sup>B. T. Gravely and J. D. Memory, Phys. Rev. B 3, 3426 (1971).
- <sup>35</sup>G. W. Parker and F. Lado, Phys. Rev. B 8, 3081 (1973).
- <sup>36</sup>G. W. Parker and F. Lado, Phys. Rev. B 9, 22 (1974).
- <sup>37</sup>J. G. Powles and B. Carazza, in *Proceedings of the Conference on Magnetic Resonance, Monash*, 1969 (Plenum, New York, 1970).
- <sup>38</sup>J. G. Powles and B. Carazza, J. Phys. A 3, 335 (1970).
- <sup>39</sup>M. Mehring, R. G. Griffin, and J. S. Waugh, J. Chem. Phys. 55, 746 (1971).
- <sup>40</sup>P. Van Hecke, J. C. Weaver, B. L. Neff, and J. S. Waugh, J. Chem. Phys. 60, 1668 (1974).
- <sup>41</sup>U. Haebleren, J. D. Ellett, Jr. and J. S. Waugh, J. Chem. Phys. 55, 53 (1971).
- <sup>42</sup>C. P. Slichter and W. C. Holton, Phys. Rev. 122, 1701 (1961).
- <sup>43</sup>A. G. Redfield, Phys. Rev. 98, 1787 (1955).
- <sup>44</sup>N. Bloembergen and P. P. Sorkin, Phys. Rev. 110, 865 (1958).
- <sup>45</sup>J. R. Franz and C. P. Slichter, Phys. Rev. 148, 287 (1966).
- <sup>46</sup>M. Kunitomo, J. Phys. Soc. Jpn. 30, 1059 (1971).
- <sup>47</sup>U. Haebleren and J. S. Waugh, Phys. Rev. 175, 453 (1968).
- <sup>48</sup>A. Pines and J. S. Waugh, Phys. Lett. A 47, 337 (1974).
- <sup>49</sup>R. Zwanzig, J. Chem. Phys. 33, 1338 (1960).
- <sup>50</sup>R. Zwanzig, *Lectures in Theoretical Physics* (University of Colorado, Boulder, 1960), Vol. 3, pp. 106.
- <sup>51</sup>P. N. Argyres and P. L. Kelley, Phys. Rev. 134, A 93 (1964).
- <sup>52</sup>H. Mori, Prog. Theor. Phys. 33, 423 (1965).
- <sup>53</sup>B. Robertson, Phys. Rev. 144, 151 (1966).
- <sup>54</sup>B. Robertson, Phys. Rev. 153, 391 (1967).
- <sup>55</sup>T. Shimizu, J. Phys. Soc. Jpn. 28, 811 (1970).
- <sup>56</sup>T. Shimizu, J. Phys. Soc. Jpn. 28, 790 (1970).
- <sup>57</sup>L. Müller, A. Kumar, T. Baumann, and R. R. Ernst, Phys. Rev. Lett. 32, 1902 (1974).
- <sup>58</sup>U. Fano, Rev. Mod. Phys. 29, 74 (1957).
- <sup>59</sup>W.-K. Rhim, A. Pines, and J. S. Waugh, Phys. Rev. B 3, 684 (1971).
- <sup>60</sup>J. F. Jacquinot, W. Th. Wenckebach, M. Goldman, and A. Abragam, Phys. Rev. Lett. 32, 1096 (1974).
- <sup>61</sup>R. Blinc, J. Pirs, and S. Zumer, Phys. Rev. B 8, 15 (1973).
- <sup>62</sup>D. Kivelson and K. Ogan, Adv. Magn. Reson. 7, 71 (1974).
- <sup>63</sup>D. E. Barnaal and I. J. Lowe, Phys. Rev. B 1, 53 (1966).
- <sup>64</sup>J. S. Waugh, in *Proceedings of the First Specialized Colloque Ampère, Krakow*, 1973 (Institute of Nuclear Physics, Krakow, Poland, 1973).
- <sup>65</sup>R. G. Gordon, J. Math. Phys. 9, 655 (1968).
- <sup>66</sup>O. Platz and R. G. Gordon, Phys. Rev. Lett. 30, 264 (1973).
- <sup>67</sup>O. Platz and R. G. Gordon, Phys. Rev. B 7, 4764 (1973).
- <sup>68</sup> $T_{1\rho}$ , in the case of spin-locking off resonance, depends on several parameters, including the rf field strength and displacement from resonance and the characteristic Zeeman relaxation times  $T_{1Z}$  and  $T_{1X}$  as described by Goldman (Ref. 14).